Roles for the *Synechococcus elongatus* RNA binding protein Rbp2 in regulating the circadian clock

Briana M. McKnight[a,b], Shannon Kang[a,b], Tam H. Le[c], Mingxu Fang[b], Genelyn Carbonel[c], Esbeydi Rodriguez[c], Sutharsan Govindarajan[d,e], Nitsan Albocher-Kedem[d], Amanda L. Tran[c], Nicholas R. Duncan[c], Orna Amster-Choder[d], Susan S. Golden[a,b*] and Susan E. Cohen[b,c*]

[a]Department of Molecular Biology, University of California, San Diego, La Jolla, CA 92093

[b]Center for Circadian Biology, University of California, San Diego, La Jolla, CA 92093

[c]Department of Biological Sciences, California State University, Los Angeles, Los Angeles, CA 90032

[d]Department of Microbiology and Molecular Genetics, IMRIC, The Hebrew University Faculty of Medicine, Jerusalem 91120, Israel

[e]Department of Biological Sciences, SRM University AP, Amaravati, India

Running title: Roles for Rbp2 in the circadian clock

Keywords: Cyanobacteria, circadian, KaiC, RNA binding protein, Rbp2

*Corresponding author: Susan S. Golden (sgolden@ucsd.edu), Division of Biological Sciences, 9500 Gilman Dr. #0116, AP&M 4721, La Jolla, CA 92093-0116. Phone: 858-246-0658 and Susan E. Cohen (scohen8@calstatela.edu), Department of Biological Sciences, 5151 State University Drive, Los Angeles, CA 90032; Phone: 323-343-2091; Fax: 323-343-6451

ABSTRACT

The cyanobacterial circadian oscillator, consisting of KaiA, KaiB and KaiC proteins, drives global rhythms of gene expression and compaction of the chromosome, and regulates the timing of cell division and natural transformation. While the KaiABC posttranslational oscillator can be reconstituted *in vitro*, the Kai-based oscillator is subject to several layers of regulation *in vivo*. Specifically, the oscillator proteins undergo changes in their subcellular localization patterns, where KaiA and KaiC are diffuse throughout the cell during the day and localized as a focus at or near the pole of the cell at night. Here we report that the CI domain of KaiC, when in a hexameric state, is sufficient to target KaiC to the pole. Moreover, increased ATPase activity of KaiC correlates with enhanced polar localization. We identified proteins associated with KaiC in either a localized or diffuse state. We found that loss of Rbp2, found to be associated with localized KaiC, results in decreased incidence of KaiC localization and long-period circadian phenotypes. Rbp2 is an RNA binding protein, and it appears that RNA binding activity of Rbp2 is required to execute clock functions. These findings uncover previously unrecognized roles for Rbp2 in regulating the circadian clock and suggest that the proper localization of KaiC is required for a fully functional clock *in vivo.*

INTRODUCTION

Circadian rhythms, regulated by a 24-h biological clock, enable the coordination of

temporal programs of cellular physiology and facilitate adaptation to daily environmental

changes in diverse organisms (Bell-Pedersen et al., 2005). Cyanobacteria are currently the only

prokaryotic system in which the molecular details of the circadian clock have been elucidated,

with *Synechococcus elongatus* PCC 7942 serving as the premier model system for the study of

the cyanobacterial circadian clock (Kondo et al., 1993). In *S. elongatus*, a core oscillator encoded

by the *kaiA*, *kaiB* and *kaiC* genes regulates global patterns of gene expression (Ishiura et al.,

1998; Kondo et al., 1994), compaction of the chromosome (Smith & Williams, 2006; Woelfle,

Xu, Qin, & Johnson, 2007), and the timing of cell division (Cohen & Golden, 2015; Dong et al.,

2010; Mori, Binder, & Johnson, 1996) and natural transformation (Taton et al., 2020). KaiC is a

hexameric protein consisting of CI and CII domains that possess autokinase and autophosphatase

(CII), and ATPase activities (both) (Nishiwaki et al., 2004; Xu et al., 2004). Rhythmic

associations of KaiA and KaiB with KaiC drive ~24-h rhythms of KaiC phosphorylation and

dephosphorylation on neighboring Serine 431 and Threonine 432 residues located in the CII

domain (Nishiwaki et al., 2004; Xu et al., 2004). During the day, KaiA associates with the A-

loops of KaiC, found on the CII domain, promoting KaiC's autokinase activity (Kim, Dong,

Carruthers, Golden, & LiWang, 2008). Once in a fully phosphorylated state, a KaiB binding site

is exposed on the CI domain of KaiC (Chang et al., 2015; Chang, Kuo, Tseng, & LiWang, 2011).

Additionally, KaiB must switch from a tetrameric ground-state fold to a monomeric fold-

switched form that is competent to bind to KaiC (Chang et al., 2015). Once both of these criteria

are met, KaiB binds to KaiC and sequesters KaiA in an autoinhibited state, triggering the

autophosphatase activity of KaiC at night (Chang et al., 2015; Tseng et al., 2017). Remarkably,

these oscillations of KaiC phosphorylation can be reconstituted *in vitro* solely with purified

KaiA, KaiB, KaiC and ATP (Nakajima et al., 2005).

These endogenously generated rhythms are synchronized with the environment through

an input pathway that monitors changes in cellular redox. Specifically, CikA, which also plays

key roles in circadian output, and KaiA directly bind oxidized quinones, whose redox status

varies as a function of photosynthetic activity, and signal the onset of darkness (Kim, Vinyard,

Ananyev, Dismukes, & Golden, 2012; Wood et al., 2010). Additionally, a drop in the ATP:ADP

ratio in the cell can reset the phase of KaiC phosphorylation directly and functions to signal the

duration of the dark period in *S. elongatus* (Rust, Golden, & O'Shea, 2011). Clock-controlled

activities are regulated by histidine kinase SasA and its cognate response regulator RpaA, as well

as CikA, which also functions as a phosphatase on RpaA (Gutu & O'Shea, 2013; Takai et al.,

2006). Association with KaiC or the KaiABC ternary complex promotes the activities of SasA

and CikA, respectively, resulting in rhythmic phosphorylation of RpaA (Gutu & O'Shea, 2013),

which in turn promotes global rhythms of gene expression (Markson, Piechura, Puszynska, &

O'Shea, 2013) and the timing of cell division (Mori et al., 1996; Yang, Pando, Dong, Golden, &

van Oudenaarden, 2010).

While several aspects of the clock can be reconstituted *in vitro*, including rhythms of

KaiC phosphorylation (Nakajima et al., 2005) as well as RpaA phosphorylation and rhythmic

DNA binding (Chavan et al., 2021), the clock *in vivo* is subject to many additional layers of

regulation. Rhythms of KaiB and KaiC protein abundance are observed, where peak expression

is achieved after dusk (Kitayama, Iwasaki, Nishiwaki, & Kondo, 2003), and the over- or under-

expression of any of the *kai* genes results in loss of rhythmicity (Ishiura et al., 1998; Xu et al.,

2013). Moreover, the clock undergoes an elegant reorganization in its subcellular localization

where KaiA and KaiC are diffuse throughout the cell during the day and become highly localized as discrete foci near a single pole of cells at night, in a clock-dependent fashion (Cohen et al., 2014). KaiA localization is dependent on KaiC, and KaiA and KaiC co-localize with CikA at night (Cohen et al., 2014). CikA is constitutively localized to the cell pole, where polar localization is observed at all circadian times (Cohen et al., 2014; Zhang, Dong, & Golden, 2006). While it is not understood how or why the clock proteins exhibit these rhythms in their subcellular localization patterns, these movements have been proposed to contribute to the robustness and synchronization of the circadian clock.

Here we report that the CI domain of KaiC is sufficient to support KaiC localization to cell poles and that the ATPase activity of KaiC correlates with the extent of polar localization. We identified proteins that associate specifically with either cytoplasmic or localized mutant variants of KaiC. Specifically, we focus on the RNA binding protein, Rbp2. We found that deletion of *rbp2* results in a long circadian period and reduced polar localization of KaiC, demonstrating that Rbp2 represents a previously unidentified component of the extended clock network. Additionally, we demonstrate that Rbp2 is the only RNA recognition motif (RRM) domain-containing protein encoded in the *S. elongatus* genome to be involved in clock regulation. We present evidence that the RNA binding activities of Rbp2 are critical for the role that Rbp2 plays in regulating the clock. The results suggest that new components of the extended clock network can be identified that are important for clock function *in vivo*, and reveal previously unrecognized roles for an RNA binding protein in regulating clock function.

MATERIALS AND METHODS

Bacterial Strains, Growth Conditions and DNA Manipulations

Plasmids and *Escherichia coli* and *S. elongatus* strains are described in Supplementary Tables 1-2. *S. elongatus* strains were grown as previously described (Clerico, Ditty, & Golden, 2007). Briefly, strains were grown in BG-11 media with the appropriate antibiotics (Taton et al., 2014). Antibiotics used in this study include chloramphenicol (Cm), kanamycin (Km), Spectinomycin and Streptomycin (Sp and Sm), gentamycin (Gm) and nourseothricin (Nt), concentrations were used as previously described (Taton et al., 2014). Plasmids were designed using the CYANO-VECTOR assembly portal (http://golden.ucsd.edu/CyanoVECTOR/), constructed with the GeneArt Seamless Cloning and Assembly Kit (Life Technologies) and propagated in *E. coli* XL1 Blue cells as previously described (Taton et al., 2014). Complementation and expression strains were constructed by expressing genes in one of three *S. elongatus* neutral sites (NS) NS1, NS2, or NS3. For the construction of knock-out strains, complete segregation of the mutant loci was verified by PCR. Point mutants were constructed using the QuickChange (Stratagene California) protocol with clones verified by Sanger sequencing.

Immunoprecipitation and Mass Spectrometry

S. elongatus cells (5×10^9) were harvested and lysed via bead beating as previously described (Ivleva & Golden, 2007) in buffer containing PBS, 1 mM phenylmethylsulphonyl fluoride (PMSF) and protease inhibitor cocktail (Roche). Rabbit IgG polyclonal GFP antibody (Life Technologies) was conjugated to magnetic Protein G Dynabeads (Thermo) following the instructions of the manufacturer and incubated with the extract for 4 hours at 4°C with rotation. The beads were washed 4 times in IA buffer (50 mM NaH_2PO_4 pH 7.8, 5 mM NaCl, 0.1% TritonX-100, 1 mM PMSF, 15U/mL DNaseI, Protease inhibitor cocktail (Roche) and PhoSTOP

phosphatase inhibitor (Roche)) and three times with PBS. Protein complexes were eluted in 50

mM glycine pH 2.8.

Protein samples were diluted in TNE (50 mM Tris pH 8.0, 100 mM NaCl, 1 mM EDTA) buffer.

RapiGest SF reagent (Waters Corporation) was added to the mix to a final concentration of 0.1%

and samples were boiled for 5 min. TCEP (Tris (2-carboxyethyl) phosphine) was added to 1 mM

(final concentration) and the samples were incubated at 37°C for 30 min. Subsequently, the

samples were carboxymethylated with 0.5 mg/ml of iodoacetamide for 30 min at 37°C followed

by neutralization with 2 mM TCEP (final concentration). Proteins samples prepared as above

were digested with trypsin (trypsin:protein ratio - 1:50) overnight at 37°C. RapiGest was

degraded and removed by treating the samples with 250 mM HCl at 37°C for 1 h followed by

centrifugation at 12,000 x g for 30 min at 4°C. The soluble fraction was then added to a new tube

and the peptides were extracted and desalted using C18 desalting columns (Thermo Fisher

Scientific, PI-87782). Peptides were quantified using BCA assay and a total of 1 microgram of

peptides were injected for LC-MS analysis.

LC-MS/MS analysis was performed as previously described (Guttman et al., 2009; McCormack

et al., 1997). Trypsin-digested peptides were analyzed by ultra high pressure liquid

chromatography (UPLC) coupled with tandem mass spectroscopy (LC-MS/MS) using nano-

spray ionization. The nanospray ionization experiments were performed using a Orbitrap fusion

Lumos hybrid mass spectrometer (Thermo Fisher Scientific) interfaced with nano-scale reversed-

phase UPLC (Thermo Dionex UltiMate™ 3000 RSLC nano System) using a 25 cm, 75-micron

ID glass capillary packed with 1.7-µm C18 (130) BEH^{TM} beads (Waters corporation). Peptides

were eluted from the C18 column into the mass spectrometer using a linear gradient (5–80%) of

acetonitrile. Mass spectrometer parameters were as follows; an MS1 survey scan using the

orbitrap detector (mass range (m/z): 400-1500 (using quadrupole isolation), 120000 resolution setting, spray voltage of 2200 V, ion transfer tube temperature of 275°C, AGC target of 400000, and maximum injection time of 50 ms) was followed by data dependent scans (top speed for most intense ions, with charge state set to only include +2-5 ions, and 5 second exclusion time, while selecting ions with minimal intensities of 50000 at in which the collision event was carried out in the high energy collision cell (HCD Collision Energy of 30%), and the fragment masses were analyzed in the ion trap mass analyzer (with ion trap scan rate of turbo, first mass m/z was 100, AGC Target 5000 and maximum injection time of 35 ms). Protein identification was carried out using Peaks Studio 8.5 (Bioinformatics solutions Inc.)

Circadian Bioluminescence Monitoring

Bioluminescence was monitored using a P*kaiB*-luc firefly luciferase fusion reporter inserted into a neutral site of the *S. elongatus* chromosome at 30°C under constant light after two entrainment cycles of 12 h in the light followed by 12 h in the dark (LD12:12) to synchronize the population as previously described (Mackey, Ditty, Clerico, & Golden, 2007). Bioluminescence was monitored every 2 h using a PerkinElmer TopCount bioluminescence plate reader. Data were collected and plotted using Microsoft Excel. Data from 12 wells of each genotype were analyzed for rhythmicity, including period ± standard deviation, using the Biological Rhythms Analysis Software System (BRASS) within Microsoft Excel.

Fluorescence Microscopy and Image Analysis

Cells were placed on a pad of 1.2% agarose in BG-11 medium and covered with a coverslip. Microscopy was performed with a DeltaVision Core system (Applied Precision) with a WeatherStation attached to an Olympus IX71 inverted microscope and an Olympus Plan Apochromat 100× objective at 30 °C with tetramethyl rhodamine isocyanate (TRITC)

(EX555/EM617) and YFP (EX500/EM535) filter settings. Images were captured using a

CoolSnap HQ CCD camera (Photometrics) and deconvolved using the SoftWorx imaging

program (Applied Precision). Exposure times were limited to conditions under which we do not

observe fluorescence from wild type (WT) strains in the YFP channels to limit bleed-through

from thylakoid fluorescence (Cohen, Erb, Pogliano, & Golden, 2015). For analysis of KaiC

localization in time-course experiments, aliquots of cells were taken at designated time points

and fixed directly in BG-11 growth medium with a final concentration of 2.4% (vol/vol)

paraformaldehyde (Electron Microscopy Sciences) in 30 mM $NaPO_4$ buffer (pH 7.5) for 20 min

at room temperature before they were moved to 4°C. Images were colorized in SoftWorx and

then transferred to Photoshop (Adobe) for figure assembly. KaiC foci tracking was performed as

previously described (Cohen et al., 2014). For imaging *E. coli*, aliquots of cells were stained

with the membrane dye FM4-64 (240 ng/ml-1 µg/ml; Molecular Probes) and 4',6-diamidino-2-

phenylindole (DAPI) (0.2 µg/mL; Thermo Fisher Scientific) prior to imaging.

Generation of Homology Model

An Rbp2 homology model was generated with SWISS-Model based on the human post-catalytic

splicesome (P complex) PDB 61CZ (Zhang et al., 2019). Initial template selection from

automatically generated models were based on three criteria: minimum of 30% sequence identity

(Haddad, Adam, & Heger, 2020), conservation of key RNP residues, and the known structure of

4 beta-sheets and 2 alpha-helices for RRM domain proteins (Maris, Dominguez, & Allain, 2005).

The selected homology model was then input into GalaxyRefine2 for energy minimization of the

protein fold via CASP algorithm (Lee, Heo, & Seok, 2018; Lee, Won, Heo, & Seok, 2019). The

refined homology model was selected from the ten likeliest proposed models based on scores

including energy, molprobity validation, root mean squared deviation, clash score, number of

poor rotamers, and Ramachandran score (Lee et al., 2018; Lee et al., 2019). RNA was manually modeled via PyMOL. The RNA sequence was determined based on the likeliest interaction of RNA bases and corresponding amino acids (Kligun & Mandel-Gutfreund, 2015).

Protein Purification and Gel Filtration Analysis

E. coli XL1 blue strain carrying pLA0004 was used to overexpress Strep-tagged Rbp2 (Rbp2-Strep) protein from a P$_{trc}$ promoter. A 20-ml overnight *E. coli* starter culture in LB medium was transferred to 1-L LB medium supplemented with 20 μg/ml spectinomycin plus 20 μg/ml streptomycin and grown to OD$_{600}$ ~0.4 at 37°C before induction with 0.2 mM isopropyl β-D-1-thiogalactopyranoside (IPTG) overnight at 22°C. *E. coli* cells were collected by centrifugation and resuspended in Strep-Tactin wash buffer (50 mM Tris pH 8.0, 150 mM NaCl, 5% glycerol) before cell lysis with an Avestin C3 Emulsiflex homogenizer (Avestin Inc, Canada). Clarified cell lysate was loaded onto a Strep-Tactin XT Superflow (IBA Lifesciences) gravity column equilibrated with Strep-Tactin wash buffer. The column was then washed with Strep-Tactin wash buffer, followed by protein elution with the same buffer containing 50 mM biotin. Rbp2-containing eluents were concentrated using spin concentrators and loaded onto a prep-grade Superdex 200 column equilibrated in a buffer containing 50 mM Tris pH 8.0, 150 mM NaCl and 5% glycerol for further purification with gel filtration chromatography. The purification of KaiC was performed as previously reported (Tseng et al., 2017).

Binding reactions were set up with different combinations of 25 μM KaiC, Rbp2 or poly(rU) (20-mer ordered from Integrated DNA Technologies) in clock buffer (20 mM Tris pH 8.0, 150 mM NaCl, 5 mM MgCl$_2$, 0.5 mM EDTA and 1 mM ATP) at 30°C. After 30 min incubation, 100 μl of the reaction mix was injected to an analytical grade Superdex 200 column equilibrated with the same clock buffer for gel filtration chromatography at room temperature with 1 ml/min flowrate.

RESULTS

CI domain of KaiC is sufficient to support KaiC polar localization

In order to investigate whether a particular domain of KaiC is necessary to support polar localization, we expressed YFP-fusions to either the full-length as well as isolated CI or CII domains of KaiC. Previous studies demonstrated that a YFP-KaiC fusion protein is functional and expressed as a full length protein (Cohen et al., 2014) and (Figure 1A). We observed that expression of the CI domain alone supports polar localization, whereas expression of the CII domain alone does not, as diffuse localization was observed (Figure 1B and 1C). When the CII domain only was overexpressed from the P_{trc} promoter by the addition of inducer IPTG, 6% of cells showed polar localization compared to 96% of cells for the full-length KaiC construct. As the CI and CII domains of KaiC are known form hexamers *in vitro* (Chang et al., 2011), we aimed to determine if the CI domain of KaiC is in a hexameric state when localized to the cell poles. We introduced mutations that substitute Ala for Arg at position 40 (R40A) and for Lys at position 172 (K172A), known to result in monomeric CI domain proteins *in vitro* (Tseng et al., 2013), into the YFP-CI domain fusion protein. We observed that monomeric CI-domain of KaiC was unable to support polar KaiC localization (Figure 1D), supporting the notion that the CI domain of KaiC needs to be in a hexameric form to be able to localize to the cell pole.

High ATPase activity correlates with enhanced KaiC polar localization

The CI domain of KaiC possesses ATPase activity that is separate from the ATPase in the CII domain required for autophosphorylation, and both domains are required for a functional clock. Although the ATPase is weak, consuming only about 15 molecules of ATP per day, it is temperature compensated and its activity oscillates in the presence of KaiA and KaiB (Terauchi et al., 2007). Approximately 70% of KaiC ATPase is attributable to the CI domain (Murakami et

al., 2008; Terauchi et al., 2007). It is proposed that the CI ATPase activity is important for inducing structural changes that regulates the timing and recruitment of KaiB (Mutoh, Nishimura, Yasui, Onai, & Ishiura, 2013). Moreover, this ATPase activity of KaiC is correlated with circadian period, leading to the hypothesis that reduced ATPase activity results in longer circadian periods and enhanced ATPase activity results in shorter circadian periods (Terauchi et al., 2007). As the CI domain of KaiC is sufficient to promote KaiC polar localization, we sought to determine whether the ATPase activity of KaiC correlates with polar localization. We tested this hypothesis by making several mutations known to alter the ATPase activity of KaiC (Dong et al., 2010; Terauchi et al., 2007) within the full length KaiC fluorescent fusion and assessing KaiC localization at Zeitgeber time (ZT) 20, representing 8 hours after the onset of darkness. These reporter strains were sampled in a light:dark cycle, rather than in constant light, because many of the mutant variants have altered or nonfunctional circadian clocks. Specifically we tested seven mutant strains whose ATPase activity is altered compared to the wild type (WT). KaiC localization was compared among: mutant variants A251V and T42S, which have longer circadian periods and reduced ATPase activity compared to WT, and S157P, F470Y and R393C, which have shorter circadian periods and elevated ATPase activity compared to WT, (Terauchi et al., 2007); KaiC-AA, in which mutation of phosphorylation sites S431 and T432 to alanine results in arrhythmia (Nishiwaki et al., 2004) and elevated ATPase activity (Terauchi et al., 2007); CI- catalytic mutant E77Q, E78Q which exhibits arrhythmia (Phong, Markson, Wilhoite, & Rust, 2013) and decreased ATPase activity (Kitayama, Nishiwaki-Ohkawa, Sugisawa, & Kondo, 2013); and WT. We observed that higher ATPase activity is correlated with higher incidence of KaiC polar localization (Figure 2). The KaiC ATPase mutants used represent changes to the combined activity of the CI and CII domains. Thus, we can conclude that KaiC

polar localization is correlated with ATPase activity of KaiC, but not necessarily with CI specific ATPase activity.

Identification of proteins that interact with KaiC in a specific localization state

Although a wide variety of cellular components in bacteria are targeted to cell poles, including those involved in chromosome segregation, chemotactic signaling, and motility, the mechanisms that establish polar recognition remain poorly understood (Davis & Waldor, 2013; Laloux & Jacobs-Wagner, 2013). Similarly, the mechanism that drives rhythms of KaiC polar localization remains elusive, although we previously determined that polar localization is not due to the formation of inclusion bodies or recruitment by the ClpXP protease (Cohen et al., 2014). Moreover, we determined that polar localization is not determined by nucleoid occlusion, membrane potential, recruitment by polar Co-ordinators/Anchors/Transporters or the by the Min system (Figure 3). We previously showed that the mechanism of KaiC localization is conserved in *E. coli,* as *S. elongatus* KaiC localizes to the pole when expressed in *E. coli* (Cohen et al., 2014). To determine whether nucleoid occlusion is involved in KaiC localization we used a strain of *E. coli* expressing the *dnaN159* temperature-sensitive allele. When shifted to the restrictive temperature the chromosome condenses, creating large nucleoid-free regions (Sutton, 2004). We found that KaiC remains localized as discrete foci even when large nucleoid-free regions are induced (Figure 3A-3B), indicating that nucleoid occlusion is not playing a role in promoting KaiC localization. We also tested whether membrane potential is involved in the subcellular localization of KaiC by treating *S. elongatus* cells with either pore former Nisin (Wiedemann et al., 2001) or the uncoupling agent 2,4-dinitrophenol (DNP) (Gage & Neidhardt, 1993); in both cases KaiC remained localized to the cell poles (Figure 3C-3E). We also tested KaiC polar localization in mutants deleted for SynPCC7942_1816 or SynPCC7942_1310, which

are homologues of *E. coli* genes that encode proteins that we named polar CATs (Coordinators/Anchors/ Transporters) because they positively affect localization of other proteins to the cell poles (see Supplemental Text and Supplementary Figures 1-2). KaiC remained at the poles in cells deleted for these genes (Figure 3F and 3G), implying that they are not important for its localization to the pole. Lastly, we sought to determine whether the Min system is involved in KaiC polar localization by assaying for KaiC localization in various *min* mutants. We observed that KaiC remains localized to the cell poles when either *minC* (Figure 3H), *minD1* (Figure 3I), *minD2* (Figure 3J) or both *minD1* and *minD2* are deleted (Figure 3K), indicating that the Min system is not involved in localizing KaiC to the poles of cells.

In order to discover unrecognized mechanisms of KaiC localization we took an unbiased approach by searching for interacting proteins through immunoprecipitation and mass spectrometry. We sought to identify factors that might be required to either target KaiC to the pole at night or sequester KaiC in the cytosol during the day, by identifying proteins that interact with KaiC preferentially in either a localized or diffuse state through the use of mutant variants. KaiC-AA, which carries a substitution of the rhythmically phosphorylated serine and threonine with alanine, has high ATPase activity and displays constitutive polar localization, whereas KaiC-AE, which carries a substitution of the phosphorylated serine and threonine with alanine and glutamic acid, respectively, a phosphomimetic of the phospho-threonine state, is constitutively hypo-localized and found primarily in the cytosol (Cohen et al., 2014). We performed immunoprecipitation experiments by capturing the YFP of the YFP-KaiC fusions as well as a free YFP control. Mass spectrometry analysis identified 22 proteins that interact specifically with localized KaiC-AA and not with KaiC-AE or free YFP, and 7 proteins that

interact with diffuse KaiC-AE and not KaiC-AA or free YFP (Supplementary Table 3), for a total of 29 proteins.

From this initial set of 29 proteins, we successfully disrupted genes encoding 11 of them and tested the resulting mutant strains for alterations in rhythms of gene expression or KaiC localization. The remaining targets represent essential genes and a knockout or insertion mutant could not be generated. We observed that the disruption of two genes, SynPCC7942_0417 and SynPCC7942_1999, whose products both associated with localized KaiC-AA, altered both rhythms of gene expression and KaiC localization compared to the WT. SynPCC7942_0417 is an unannotated gene whose sequence suggests that it encodes a member of the AAA+ family of ATPases. Disruption of SynPCC7942_0417 led to an approximately one hour longer period compared to the WT (Supplementary Figure 3) and a mild reduction in KaiC localization at night (Figure 4A). Interestingly, protein localization prediction tools suggest that SynPCC7942_0417 displays cytoplasmic membrane localization, similar to the cell division protease FtsH, which is also a member of the AAA+ family of ATPases (Gardy et al., 2003). However, here we focus on SynPCC7942_1999, which encodes the Rbp2 protein. As neither of these genes has been previously implicated in circadian rhythms, they represent novel avenues for understanding how the clock functions *in vivo*.

Deletion of *rbp2* results in changes to the circadian clock

Rbp2 is an RNA binding protein that contains a single RNA recognition motif (RRM). RRM domain-containing proteins are most commonly found in eukaryotes, with only 85 proteins identified in bacteria, most of which are cyanobacteria (Maruyama, Sato, & Ohta, 1999). In eukaryotes, RRM-domain proteins are involved in all aspects of post-translational regulation; however, their roles in bacteria remain unclear (Maris et al., 2005). We found that deletion of

rbp2 (Δ*rbp2*) results in an approximate 50% reduction in KaiC localization at night (Figure 4A), and an ~1.5 hour longer period, which can be complemented by expressing *rbp2* from a neutral site under its native promoter (Figure 4B). Taken together these data suggest that Rbp2 plays a role in regulating the circadian clock and supports the notion that the proper localization of KaiC is important for WT clock function.

Rbp2 is the only RRM-domain protein involved in the circadian clock

The *S. elongatus* genome encodes three RRM-domain proteins: Rbp1, Rbp2 and Rbp3. Rbp1 consists of an RRM domain followed by a glycine-rich domain, while Rbp2 consists solely of a single RRM domain, and Rbp3 contains an RRM domain followed by a conserved PDPRWA motif in the C-terminus (Figure 5A). The Rbp proteins were initially proposed to have a similar function to the cold-shock RNA chaperones of other bacteria, promoting translation at low temperatures (C. Sugita, Mutsuda, Sugiura, & Sugita, 1999), because clear homologs of the canonical bacterial cold-shock RNA chaperones are not present in *S. elongatus*. Indeed, Rbp1 is induced by cold shock and promotes survival under low temperatures (Mutsuda, Sugiura, & Sugita, 1999; C. Sugita et al., 1999). However, neither Rbp2 nor Rbp3 is induced by low temperatures nor does either contribute to cellular survival at low temperatures (Hayashi, Sugita, & Sugita, 2017; C. Sugita et al., 1999). Additionally, Rbp1 and Rbp2 have been verified experimentally to bind RNA *in vitro* (M. Sugita & Sugiura, 1994). While the roles for Rbp1 in promoting survival in response to cold stress seem clear, the functions of Rbp2 (and Rbp3) in the cell remain elusive.

In order to determine whether Rbp2 is the only RRM-domain protein involved in clock function, we generated strains that lack each of the *rbp* genes as well as all combinations of pairwise deletions. We were unable to generate the triple mutant strain, suggesting that the *rbp*

genes likely have some overlapping function that is required for viability. Additionally, we found that while Δ*rbp1* strains are viable, they could not be maintained for long periods of time. We found that only strains lacking *rbp2*, both single- and double-mutant strains (Δ*rbp1*Δ*rbp2* and Δ*rbp2*Δ*rbp3*), displayed any circadian phenotypes, where the loss of *rbp2* resulted in a 1-1.5 h longer circadian period of gene expression (Figure 5B-5C). These data suggest that while the three Rbp proteins may have some overlapping function, Rbp2 is the only RRM-domain protein that is involved in clock function.

RNA binding activity of Rbp2 is likely involved in regulation of the circadian clock

As Rbp2 consists solely of an RRM domain that has been biochemically verified to bind RNA (M. Sugita & Sugiura, 1994), we sought to determine whether the RNA binding activity is required for its roles in regulating the circadian clock. The RRM domain forms an αβ sandwich structure that consists of subdomains RNP 1, located in the C-terminus, and RNP 2, located in the N-terminus. Four conserved hydrophobic residues in these motifs contribute to RNA binding (Maris et al., 2005). We generated a homology model of Rbp2 based on published structures of eukaryotic RRM domains and found that Tyrosine 4, located in RNP 2, and Arginine 42, Phenylalanine 44 and Phenylalanine 46, located in RNP 1, of Rbp2 are similarly poised to coordinate binding to RNA (Figure 6A). We mutated these conserved amino acids to alanine in order to generate strains expressing *rbp2-Y4A* or *rbp2-R42A-F44A-F46A*. We found that expression of these mutant variants, predicted to have reduced ability to bind to RNA, does not complement the *rbp2* null strain, where long-period circadian rhythms of gene expression are observed (Figure 6B). These data suggest that the RNA binding activities of Rbp2 are necessary for it to execute its effect on the circadian clock.

Rbp2 and KaiC likely interact indirectly

To determine whether Rbp2 is associating with KaiC directly or indirectly we performed gel filtration analysis. After a 30 min incubation of purified Rbp2 and KaiC no Rbp2-KaiC complex was observed, suggesting that these two proteins do not interact directly *in vitro* (Figure 7A- 7C). As Rbp2 is known to bind to single-stranded RNA, specifically poly(U) and poly(G) RNA homopolymers (M. Sugita & Sugiura, 1994), and RNA binding activity of Rbp2 appears to be required for it to execute clock function (Figure 6B), we sought to determine if an association between Rbp2 or KaiC could be detected in the presence of RNA. We were able to confirm that Rbp2 binds to poly(U) RNA (poly(rU)) (Figure 7D- 7E); however, an association between KaiC and Rbp2 was not observed after a 30 min incubation with purified KaiC, Rbp2, and poly(rU) (Figure 7E- 7G). While it remains possible that Rbp2 and KaiC interact directly under conditions that were not tested, these data suggest that Rbp2 does not interact directly with KaiC and that other proteins are likely required to associate Rbp2 with KaiC.

DISCUSSION

Both the mechanism and function of KaiC temporal localization remain unclear, although the discovery that Rbp2 affects this process provides new avenues for investigation. Because these two proteins do not show evidence of direct interaction *in vitro*, it is possible that Rbp2 bound to RNA creates a scaffold at or near the poles of cells, allowing for the docking or association of clock proteins. Such organization could potentially allow for clock complexes to associate at the appropriate stoichiometry and/or promote KaiC monomer shuffling, in which monomers are exchanged among KaiC hexamers. Monomer shuffling occurs during the dephosphorylation phase of the cycle and contributes to synchronization and stability of the Kai oscillator (Ito et al., 2007; Kageyama et al., 2006). Without this scaffold, it is possible that it

would take longer for the complexes to assemble leading to the observed long-period rhythms in gene expression.

We found that the CI domain of KaiC is sufficient to promote KaiC polar localization and that enhanced ATPase activity of KaiC correlates with enhanced polar localization. These data are consistent with the observations that ATPase activity of KaiC as well as its localization increase throughout the nighttime period (Cohen et al., 2014; Terauchi et al., 2007). Although the CI and CII domains are very similar, CI showed much higher propensity to localize. The hexamerization of CII is known to vary depending on phosphorylation state (Chang et al., 2011), which has not been characterized *in vivo* for the single domain. The recovery of CII polar localization upon overexpression may reflect a concentration-driven hexamerization that otherwise is unlikely to occur when the domain is expressed alone. Taken together, these data could suggest that the conformation of KaiC that promotes enhanced ATPase activity may also promote localization to the pole, perhaps by allowing for the binding of a partner that recruits KaiC to the pole.

We report that both the ATPase activity of KaiC and Rbp2 are involved in the localization of KaiC to one pole of the cell at night. Given the absence a direct interaction between KaiC and Rbp2 *in vitro* it is possible that KaiC ATPase and Rbp2 activities represent independent mechanisms that promote KaiC polar localization. However, it is also possible that they are connected. KaiC has enhanced ATPase activity when in association with KaiB and CikA (Mutoh et al., 2013; Tseng et al., 2017). It is possible that these proteins are responsible for associating with Rbp2, and only once this clock complex has been assembled do we observe WT rhythmicity *in vivo*.

Intriguingly, RRM-domain proteins similar to the one identified here have been reported to play roles in the circadian clock in eukaryotes. Clock-controlled RRM-containing proteins have been identified in the eukaryotic microalgae *Gonyaulax* and *Chlamydomonas reinhardtii* as well as *Neurospora, Arabidopsis* and *Drosophila* (Mittag, 2003; Schroeder et al., 2003; Staiger, 2001; Zhao et al., 2004). In *Drosophila*, the RRM-domain containing protein LARK exhibits rhythms in abundance (McNeil, Zhang, Genova, & Jackson, 1998) and its knock-down results in arrhythmic locomotor activity (Sundram et al., 2012). Moreover, abundance of the RNA binding protein AtGRP7 of *Arabidopsis thaliana* oscillates with circadian rhythmicity and overexpression represses these oscillations, suggesting it is part of a negative regulatory loop (Heintzen, Nater, Apel, & Staiger, 1997). The precise roles that these factors play in circadian function have not been determined, but they have all been proposed to function in circadian output and information relay from the oscillator to circadian controlled behaviors. While clock-controlled RRM-domain proteins have been implicated in circadian function in many different eukaryotic models, this report of RNA binding activities or an RRM-domain protein in the prokaryotic clock model system suggests a novel conserved mechanism by which circadian clocks are regulated.

ACKNOWLEDGMENTS

REFERENCES

Arnold, C., & Hodgson, I. J. (1991). Vectorette PCR: a novel approach to genomic walking. *PCR Methods Appl, 1*(1), 39-42. doi:10.1101/gr.1.1.39

Bell-Pedersen, D., Cassone, V. M., Earnest, D. J., Golden, S. S., Hardin, P. E., Thomas, T. L., & Zoran, M. J. (2005). Circadian rhythms from multiple oscillators: lessons from diverse organisms. *Nat Rev Genet, 6*(7), 544-556.

Chang, Y. G., Cohen, S. E., Phong, C., Myers, W. K., Kim, Y. I., Tseng, R., . . . LiWang, A. (2015). A protein fold switch joins the circadian oscillator to clock output in cyanobacteria. *Science, 349*(6245), 324-328. doi:science.1260031 [pii]10.1126/science.1260031

Chang, Y. G., Kuo, N. W., Tseng, R., & LiWang, A. (2011). Flexibility of the C-terminal, or CII, ring of KaiC governs the rhythm of the circadian clock of cyanobacteria. *Proc Natl Acad Sci U S A, 108*(35), 14431-14436. doi:1104221108 [pii]10.1073/pnas.1104221108

Chavan, A. G., Swan, J. A., Heisler, J., Sancar, C., Ernst, D. C., Fang, M., . . . LiWang, A. (2021). Reconstitution of an intact clock reveals mechanisms of circadian timekeeping. *Science, 374*(6564), eabd4453. doi:10.1126/science.abd4453

Clerico, E. M., Ditty, J. L., & Golden, S. S. (2007). Specialized techniques for site-directed mutagenesis in cyanobacteria. *Methods Mol Biol, 362*, 155-171. doi:1-59745-257-2:155 [pii]10.1007/978-1-59745-257-1_11

Cohen, S. E., Erb, M. L., Pogliano, J., & Golden, S. S. (2015). Best practices for fluorescence microscopy of the cyanobacterial circadian clock. *Methods Enzymol, 551*, 211-221. doi:S0076-6879(14)00015-9 [pii]10.1016/bs.mie.2014.10.014

Cohen, S. E., Erb, M. L., Selimkhanov, J., Dong, G., Hasty, J., Pogliano, J., & Golden, S. S. (2014). Dynamic localization of the cyanobacterial circadian clock proteins. *Curr Biol, 24*(16), 1836-1844. doi:S0960-9822(14)00899-9 [pii]10.1016/j.cub.2014.07.036

Cohen, S. E., & Golden, S. S. (2015). Circadian Rhythms in Cyanobacteria. *Microbiol Mol Biol Rev, 79*(4), 373-385. doi:10.1128/MMBR.00036-15

Datsenko, K. A., & Wanner, B. L. (2000). One-step inactivation of chromosomal genes in Escherichia coli K-12 using PCR products. *Proc Natl Acad Sci U S A, 97*(12), 6640-6645. doi:10.1073/pnas.120163297

Davis, B. M., & Waldor, M. K. (2013). Establishing polar identity in Gram-negative rods. *Curr Opin Microbiol, 16*(6), 752-759. doi:S1369-5274(13)00148-3 [pii]10.1016/j.mib.2013.08.006

Ditty, J. L., Canales, S. R., Anderson, B. E., Williams, S. B., & Golden, S. S. (2005). Stability of the *Synechococcus elongatus* PCC 7942 circadian clock under directed anti-phase expression of the kai genes. *Microbiology, 151*(Pt 8), 2605-2613. doi:151/8/2605 [pii]10.1099/mic.0.28030-0

Dong, G., Yang, Q., Wang, Q., Kim, Y. I., Wood, T., Osteryoung, K. W., . . . Golden, S. S. (2010). Elevated ATPase activity of KaiC constitutes a circadian checkpoint of cell division in *Synechococcus elongatus*. *Cell, 140*(4), 529-539.

Fixen, K. R., Janakiraman, A., Garrity, S., Slade, D. J., Gray, A. N., Karahan, N., . . . Goldberg, M. B. (2012). Genetic reporter system for positioning of proteins at the bacterial pole. *MBio, 3*(2). doi:mBio.00251-11 [pii]10.1128/mBio.00251-11

Gage, D. J., & Neidhardt, F. C. (1993). Adaptation of Escherichia coli to the uncoupler of

    oxidative phosphorylation 2,4-dinitrophenol. *J Bacteriol, 175*(21), 7105-7108.

    doi:10.1128/jb.175.21.7105-7108.1993

Gardy, J. L., Spencer, C., Wang, K., Ester, M., Tusnady, G. E., Simon, I., . . . Brinkman, F. S.

    (2003). PSORT-B: Improving protein subcellular localization prediction for Gram-

    negative bacteria. *Nucleic Acids Res, 31*(13), 3613-3617. doi:10.1093/nar/gkg602

Govindarajan, S., Elisha, Y., Nevo-Dinur, K., & Amster-Choder, O. (2013). The general

    phosphotransferase system proteins localize to sites of strong negative curvature in

    bacterial cells. *MBio, 4*(5), e00443-00413. doi:10.1128/mBio.00443-13

Guttman, M., Betts, G. N., Barnes, H., Ghassemian, M., van der Geer, P., & Komives, E. A.

    (2009). Interactions of the NPXY microdomains of the low density lipoprotein receptor-

    related protein 1. *Proteomics, 9*(22), 5016-5028. doi:10.1002/pmic.200900457

Gutu, A., & O'Shea, E. K. (2013). Two antagonistic clock-regulated histidine kinases time the

    activation of circadian gene expression. *Mol Cell, 50*(2), 288-294. doi:S1097-

    2765(13)00178-0 [pii]10.1016/j.molcel.2013.02.022

Haddad, Y., Adam, V., & Heger, Z. (2020). Ten quick tips for homology modeling of high-

    resolution protein 3D structures. *PLoS Comput Biol, 16*(4), e1007449.

    doi:10.1371/journal.pcbi.1007449

Hayashi, R., Sugita, C., & Sugita, M. (2017). The 5' untranslated region of the rbp1 mRNA is

    required for translation of its mRNA under low temperatures in the cyanobacterium

    Synechococcus elongatus. *Arch Microbiol, 199*(1), 37-44. doi:10.1007/s00203-016-1270-

    0

Heintzen, C., Nater, M., Apel, K., & Staiger, D. (1997). AtGRP7, a nuclear RNA-binding protein as a component of a circadian-regulated negative feedback loop in Arabidopsis thaliana. *Proc Natl Acad Sci U S A, 94*(16), 8515-8520.

Holtman, C. K., Chen, Y., Sandoval, P., Gonzales, A., Nalty, M. S., Thomas, T. L., . . . Golden, S. S. (2005). High-throughput functional analysis of the *Synechococcus elongatus* PCC 7942 genome. *DNA Res, 12*(2), 103-115. doi:12/2/103 [pii]10.1093/dnares/12.2.103

Ishiura, M., Kutsuna, S., Aoki, S., Iwasaki, H., Andersson, C. R., Tanabe, A., . . . Kondo, T. (1998). Expression of a gene cluster *kaiABC* as a circadian feedback process in cyanobacteria. *Science, 281*(5382), 1519-1523.

Ito, H., Kageyama, H., Mutsuda, M., Nakajima, M., Oyama, T., & Kondo, T. (2007). Autonomous synchronization of the circadian KaiC phosphorylation rhythm. *Nat Struct Mol Biol, 14*(11), 1084-1088. doi:nsmb1312 [pii]10.1038/nsmb1312

Ivleva, N. B., & Golden, S. S. (2007). Protein extraction, fractionation, and purification from cyanobacteria. *Methods Mol Biol, 362*, 365-373. doi:1-59745-257-2:365 [pii]

Kageyama, H., Nishiwaki, T., Nakajima, M., Iwasaki, H., Oyama, T., & Kondo, T. (2006). Cyanobacterial circadian pacemaker: Kai protein complex dynamics in the KaiC phosphorylation cycle in vitro. *Mol Cell, 23*(2), 161-171. doi:S1097-2765(06)00381-9 [pii]10.1016/j.molcel.2006.05.039

Kim, Y. I., Dong, G., Carruthers, C. W., Jr., Golden, S. S., & LiWang, A. (2008). The day/night switch in KaiC, a central oscillator component of the circadian clock of cyanobacteria. *Proc Natl Acad Sci U S A, 105*(35), 12825-12830. doi:0800526105 [pii]10.1073/pnas.0800526105

Kim, Y. I., Vinyard, D. J., Ananyev, G. M., Dismukes, G. C., & Golden, S. S. (2012). Oxidized
quinones signal onset of darkness directly to the cyanobacterial circadian oscillator. *Proc
Natl Acad Sci U S A, 109*(44), 17765-17769. doi:1216401109
[pii]10.1073/pnas.1216401109

Kitayama, Y., Iwasaki, H., Nishiwaki, T., & Kondo, T. (2003). KaiB functions as an attenuator
of KaiC phosphorylation in the cyanobacterial circadian clock system. *EMBO J, 22*(9),
2127-2134. doi:10.1093/emboj/cdg212

Kitayama, Y., Nishiwaki-Ohkawa, T., Sugisawa, Y., & Kondo, T. (2013). KaiC intersubunit
communication facilitates robustness of circadian rhythms in cyanobacteria. *Nat
Commun, 4*, 2897. doi:ncomms3897 [pii]10.1038/ncomms3897

Kligun, E., & Mandel-Gutfreund, Y. (2015). The role of RNA conformation in RNA-protein
recognition. *RNA Biol, 12*(7), 720-727. doi:10.1080/15476286.2015.1040977

Kondo, T., Strayer, C. A., Kulkarni, R. D., Taylor, W., Ishiura, M., Golden, S. S., & Johnson, C.
H. (1993). Circadian rhythms in prokaryotes: luciferase as a reporter of circadian gene
expression in cyanobacteria. *Proc Natl Acad Sci U S A, 90*(12), 5672-5676.

Kondo, T., Tsinoremas, N. F., Golden, S. S., Johnson, C. H., Kutsuna, S., & Ishiura, M. (1994).
Circadian clock mutants of cyanobacteria. *Science, 266*(5188), 1233-1236.

Laloux, G., & Jacobs-Wagner, C. (2013). How do bacteria localize proteins to the cell pole? *J
Cell Sci, 127*(Pt 1), 11-19. doi:jcs.138628 [pii]10.1242/jcs.138628

Lee, G. R., Heo, L., & Seok, C. (2018). Simultaneous refinement of inaccurate local regions and
overall structure in the CASP12 protein model refinement experiment. *Proteins, 86 Suppl
1*, 168-176. doi:10.1002/prot.25404

Lee, G. R., Won, J., Heo, L., & Seok, C. (2019). GalaxyRefine2: simultaneous refinement of inaccurate local regions and overall protein structure. *Nucleic Acids Res, 47*(W1), W451-W455. doi:10.1093/nar/gkz288

Lopian, L., Elisha, Y., Nussbaum-Shochat, A., & Amster-Choder, O. (2010). Spatial and temporal organization of the E. coli PTS components. *EMBO J, 29*(21), 3630-3645. doi:10.1038/emboj.2010.240

Mackey, S. R., Ditty, J. L., Clerico, E. M., & Golden, S. S. (2007). Detection of rhythmic bioluminescence from luciferase reporters in cyanobacteria. *Methods Mol Biol, 362*, 115-129. doi:1-59745-257-2:115 [pii]10.1007/978-1-59745-257-1_8

Maris, C., Dominguez, C., & Allain, F. H. (2005). The RNA recognition motif, a plastic RNA-binding platform to regulate post-transcriptional gene expression. *FEBS J, 272*(9), 2118-2131. doi:10.1111/j.1742-4658.2005.04653.x

Markson, J. S., Piechura, J. R., Puszynska, A. M., & O'Shea, E. K. (2013). Circadian control of global gene expression by the cyanobacterial master regulator RpaA. *Cell, 155*(6), 1396-1408. doi:S0092-8674(13)01418-9 [pii]10.1016/j.cell.2013.11.005

Maruyama, K., Sato, N., & Ohta, N. (1999). Conservation of structure and cold-regulation of RNA-binding proteins in cyanobacteria: probable convergent evolution with eukaryotic glycine-rich RNA-binding proteins. *Nucleic Acids Res, 27*(9), 2029-2036.

McCormack, A. L., Schieltz, D. M., Goode, B., Yang, S., Barnes, G., Drubin, D., & Yates, J. R., 3rd. (1997). Direct analysis and identification of proteins in mixtures by LC/MS/MS and database searching at the low-femtomole level. *Anal Chem, 69*(4), 767-776. doi:10.1021/ac960799q

McNeil, G. P., Zhang, X., Genova, G., & Jackson, F. R. (1998). A molecular rhythm mediating circadian clock output in Drosophila. *Neuron, 20*(2), 297-303.

Mittag, M. (2003). The Function of Circadian RNA-Binding Proteins and Their *cis*-Acting Elements in Microalgae. *The Journal of Biological and Medical Rhythm Research, 20*(4), 529-541.

Mori, T., Binder, B., & Johnson, C. H. (1996). Circadian gating of cell division in cyanobacteria growing with average doubling times of less than 24 hours. *Proc Natl Acad Sci U S A, 93*(19), 10183-10188.

Murakami, R., Miyake, A., Iwase, R., Hayashi, F., Uzumaki, T., & Ishiura, M. (2008). ATPase activity and its temperature compensation of the cyanobacterial clock protein KaiC. *Genes Cells, 13*(4), 387-395. doi:10.1111/j.1365-2443.2008.01174.x

Mutoh, R., Nishimura, A., Yasui, S., Onai, K., & Ishiura, M. (2013). The ATP-mediated regulation of KaiB-KaiC interaction in the cyanobacterial circadian clock. *PLoS One, 8*(11), e80200. doi:10.1371/journal.pone.0080200PONE-D-13-10655 [pii]

Mutsuda, M., Sugiura, M., & Sugita, M. (1999). Physiological Characterization of RNA-Binding Protein-Deficient Cells from *Synechococcs* sp. Strain PCC7942. *Plant Cell Physiol, 401*(12), 1203-1209.

Nakajima, M., Imai, K., Ito, H., Nishiwaki, T., Murayama, Y., Iwasaki, H., . . . Kondo, T. (2005). Reconstitution of circadian oscillation of cyanobacterial KaiC phosphorylation in vitro. *Science, 308*(5720), 414-415.

Nishiwaki, T., Satomi, Y., Nakajima, M., Lee, C., Kiyohara, R., Kageyama, H., . . . Kondo, T. (2004). Role of KaiC phosphorylation in the circadian clock system of *Synechococcus*

elongatus PCC 7942. *Proc Natl Acad Sci U S A, 101*(38), 13927-13932. doi:10.1073/pnas.0403906101 [pii]

Phong, C., Markson, J. S., Wilhoite, C. M., & Rust, M. J. (2013). Robust and tunable circadian rhythms from differentially sensitive catalytic domains. *Proc Natl Acad Sci U S A, 110*(3), 1124-1129. doi:10.1073/pnas.1212113110

Rubin, B. E., Wetmore, K. M., Price, M. N., Diamond, S., Shultzaberger, R. K., Lowe, L. C., . . . Golden, S. S. (2015). The essential gene set of a photosynthetic organism. *Proc Natl Acad Sci U S A, 112*(48), E6634-6643. doi:10.1073/pnas.1519220112

Rust, M. J., Golden, S. S., & O'Shea, E. K. (2011). Light-driven changes in energy metabolism directly entrain the cyanobacterial circadian oscillator. *Science, 331*(6014), 220-223. doi:331/6014/220 [pii]10.1126/science.1197243

Schroeder, A. J., Genova, G. K., Roberts, M. A., Kleyner, Y., Suh, J., & Jackson, F. R. (2003). Cell-specific expression of the lark RNA-binding protein in Drosophila results in morphological and circadian behavioral phenotypes. *J Neurogenet, 17*(2-3), 139-169.

Smith, R. M., & Williams, S. B. (2006). Circadian rhythms in gene transcription imparted by chromosome compaction in the cyanobacterium *Synechococcus elongatus*. *Proc Natl Acad Sci U S A, 103*(22), 8564-8569.

Staiger, D. (2001). RNA-binding proteins and circadian rhythms in Arabidopsis thaliana. *Philos Trans R Soc Lond B Biol Sci, 356*(1415), 1755-1759. doi:10.1098/rstb.2001.0964

Sugita, C., Mutsuda, M., Sugiura, M., & Sugita, M. (1999). Targeted deletion of genes for eukaryotic RNA-binding proteins, Rbp1 and Rbp2, in the cyanobacterium *Synechococcus elongatus* sp. strain PCC7942: Rpb1 is indispensable for cell growth at low temperatures. *FEMS Microbiol Lett, 176*, 155-161.

Sugita, M., & Sugiura, M. (1994). The existence of eukaryotic ribonucleoprotein consensus sequence-type RNA-binding proteins in a prokaryote, Synechococcus 6301. *Nucleic Acids Res, 22*(1), 25-31.

Sundram, V., Ng, F. S., Roberts, M. A., Millan, C., Ewer, J., & Jackson, F. R. (2012). Cellular requirements for LARK in the Drosophila circadian system. *J Biol Rhythms, 27*(3), 183-195. doi:10.1177/0748730412440667

Sutton, M. D. (2004). The Escherichia coli dnaN159 mutant displays altered DNA polymerase usage and chronic SOS induction. *J Bacteriol, 186*(20), 6738-6748. doi:10.1128/JB.186.20.6738-6748.2004

Takai, N., Nakajima, M., Oyama, T., Kito, R., Sugita, C., Sugita, M., . . . Iwasaki, H. (2006). A KaiC-associating SasA-RpaA two-component regulatory system as a major circadian timing mediator in cyanobacteria. *Proc Natl Acad Sci U S A, 103*(32), 12109-12114. doi:0602955103 [pii]10.1073/pnas.0602955103

Taton, A., Erikson, C., Yang, Y., Rubin, B. E., Rifkin, S. A., Golden, J. W., & Golden, S. S. (2020). The circadian clock and darkness control natural competence in cyanobacteria. *Nat Commun, 11*(1), 1688. doi:10.1038/s41467-020-15384-9

Taton, A., Unglaub, F., Wright, N. E., Zeng, W. Y., Paz-Yepes, J., Brahamsha, B., . . . Golden, J. W. (2014). Broad-host-range vector system for synthetic biology and biotechnology in cyanobacteria. *Nucleic Acids Res, 42*(17), e136. doi:10.1093/nar/gku673

Terauchi, K., Kitayama, Y., Nishiwaki, T., Miwa, K., Murayama, Y., Oyama, T., & Kondo, T. (2007). ATPase activity of KaiC determines the basic timing for circadian clock of cyanobacteria. *Proc Natl Acad Sci U S A, 104*(41), 16377-16381. doi:0706292104 [pii]10.1073/pnas.0706292104

Tseng, R., Chang, Y. G., Bravo, I., Latham, R., Chaudhary, A., Kuo, N. W., & Liwang, A. (2013). Cooperative KaiA-KaiB-KaiC interactions affect KaiB/SasA competition in the circadian clock of cyanobacteria. *J Mol Biol, 426*(2), 389-402. doi:S0022-2836(13)00624-4 [pii]10.1016/j.jmb.2013.09.040

Tseng, R., Goularte, N. F., Chavan, A., Luu, J., Cohen, S. E., Chang, Y. G., . . . Partch, C. L. (2017). Structural basis of the day-night transition in a bacterial circadian clock. *Science, 355*(6330), 1174-1180. doi:10.1126/science.aag2516

Wiedemann, I., Breukink, E., van Kraaij, C., Kuipers, O. P., Bierbaum, G., de Kruijff, B., & Sahl, H. G. (2001). Specific binding of nisin to the peptidoglycan precursor lipid II combines pore formation and inhibition of cell wall biosynthesis for potent antibiotic activity. *J Biol Chem, 276*(3), 1772-1779. doi:10.1074/jbc.M006770200

Woelfle, M. A., Xu, Y., Qin, X., & Johnson, C. H. (2007). Circadian rhythms of superhelical status of DNA in cyanobacteria. *Proc Natl Acad Sci U S A, 104*(47), 18819-18824.

Wood, T. L., Bridwell-Rabb, J., Kim, Y. I., Gao, T., Chang, Y. G., LiWang, A., . . . Golden, S. S. (2010). The KaiA protein of the cyanobacterial circadian oscillator is modulated by a redox-active cofactor. *Proc Natl Acad Sci U S A, 107*(13), 5804-5809. doi:0910141107 [pii]10.1073/pnas.0910141107

Xu, Y., Ma, P., Shah, P., Rokas, A., Liu, Y., & Johnson, C. H. (2013). Non-optimal codon usage is a mechanism to achieve circadian clock conditionality. *Nature, 495*(7439), 116-120. doi:nature11942 [pii]10.1038/nature11942

Xu, Y., Mori, T., Pattanayek, R., Pattanayek, S., Egli, M., & Johnson, C. H. (2004). Identification of key phosphorylation sites in the circadian clock protein KaiC by

crystallographic and mutagenetic analyses. *Proc Natl Acad Sci U S A, 101*(38), 13933-

13938. doi:10.1073/pnas.0404768101

Yang, Q., Pando, B. F., Dong, G., Golden, S. S., & van Oudenaarden, A. (2010). Circadian

gating of the cell cycle revealed in single cyanobacterial cells. *Science, 327*(5972), 1522-

1526. doi:327/5972/1522 [pii]10.1126/science.1181759

Zhang, X., Dong, G., & Golden, S. S. (2006). The pseudo-receiver domain of CikA regulates the

cyanobacterial circadian input pathway. *Mol Microbiol, 60*(3), 658-668. doi:MMI5138

[pii] 10.1111/j.1365-2958.2006.05138.x

Zhang, X., Zhan, X., Yan, C., Zhang, W., Liu, D., Lei, J., & Shi, Y. (2019). Structures of the

human spliceosomes before and after release of the ligated exon. *Cell Res, 29*(4), 274-

285. doi:10.1038/s41422-019-0143-x

Zhao, B., Schneid, C., Iliev, D., Schmidt, E. M., Wagner, V., Wollnik, F., & Mittag, M. (2004).

The circadian RNA-binding protein CHLAMY 1 represents a novel type heteromer of

RNA recognition motif and lysine homology domain-containing subunits. *Eukaryot Cell,*

3(3), 815-825. doi:10.1128/EC.3.3.815-825.2004

FIGURE LEGENDS

Figure 1. The CI domain of KaiC is sufficient to support KaiC polar localization. Fluorescent micrographs of cells expressing A) YFP-KaiC full length fusion, B)YFP-KaiC-CI domain fusion, C) YFP-KaiC-CII domain fusion and D) YFP-KaiC-CI$^{R40A-K172A}$ monomer fusion (yellow) in a $\Delta kaiC$ background (AMC704), shows that the CI domain alone, when in a hexameric state, can localize to the cell pole while the CII domain is not capable of polar localization. When the YFP-KaiC-CII domain only construct was overexpressed, only 6% of the cells showed polar localization compared to 96% of cells in the full-length YFP-KaiC fusion. Autofluorescence is shown in red. Scale bars = 2.5 microns.

Figure 2. Increased ATPase activity is correlated with enhanced KaiC polar localization. Percentage of cells containing a KaiC focus (Y-axis) increases as ATPase activity increases (X-axis). Varying levels of ATPase activity, taken from the literature, are plotted from lowest (left) to highest (right) on the X-axis. KaiC mutant variants were expressed in a $\Delta kaiC$ background (AMC704). Strains were entrained in 12 h light:12 h dark and samples were collected at ZT20, 8 hours after the onset of darkness. Percentage of cells with foci was calculated from at least 100 cells from 3 frames. Numbers represent average ± the standard deviation from three independent experiments. Below is a schematic showing the positions of ATPase mutations used on the KaiC protein.

Figure 3. KaiC polar localization is not determined by various cellular factors. A-B) KaiC localization is not driven by nucleoid occlusion. YFP-KaiC (green) was expressed in the temperature sensitive *E. coli* strain AB1157 *dnaN159* which was diluted into fresh LB medium

and A) kept at permissive temperature (30°C) or B) shifted to the non-permissive temperature (42°C) for 2 hours to create a large nucleoid free region. Cells were stained with vital membrane FM4-64 (red) and DAPI (blue) to stain the DNA. Even when a large nucleoid free region was created, KaiC still localized as a discrete focus, indicating that nucleoid occlusion does not drive KaiC localization. Scale bar = 2.5 microns. C-D) KaiC localization is not driven by membrane potential. *S. elongatus* cells treated with either C) 0.025% DMSO control, D) 1.25 µg/mL pore former Nisin, or E) 184 µg/mL chemical uncoupler DNP show that KaiC remains localized even after membrane potential is perturbed. Autofluorescence is shown in red, except in panel E, becuase treatment with DNP resulted in loss of autofluorescence; therefore KaiC localization in E is overlaid onto the differential interference contrast (DIC) image. Scale bar = 5 microns. F-G) Polar CATs are not responsible for KaiC localization. KaiC remains localized in strains in which homologs of *E. coli* polar CATs have been mutated F) SynPCC7942_1310 and G) SynPCC7942_1816. Autofluorescence is shown in red. Scale bar = 2.5 microns. H-K) The Min system is not responsible for KaiC localization. KaiC remains localized in H) *minC* insertional mutant, I) *minD1* deletion mutant, J) *minD2* insertional mutant and K) *minD1, minD*2 double mutant. Autofluorescence is shown in red. Scale bar = 2.5 microns.

Figure 4. Disruption of *rbp2* results in altered circadian phenotypes. A) Strains expressing YFP-KaiC were entrained to opposite light-dark cycles and sampled every 2 hours, with the light (ZT 0-12) and dark (ZT 12-24) samples removed from different incubators at the same laboratory time. Zeitgeber time refers to the time relative to when the lights turn on. Deletion of *rbp2* results in an ~50% reduction (open circles), and disruption of SynPCC7942_0417 a slight reduction (triangles) compared to the WT (closed circles). WT is AMC2158 transformed with pAM5428

($\Delta kaiC$) and pAM5081 (YFP-KaiC). B) Bioluminescence output represented as counts per second from strains carrying P$_{kaiB}$-*luc* reporter. LL on X-axis refers to constant light. Deletion of *rbp2* results in long-period rhythms of gene expression, open circles (26.7 ± 0.6 h), compared with WT AMC2036, squares (25 ± 0.4 h). This defect can be rescued by expressing *rbp2* under its native promoter from NS1, triangles (25.3 ± 0.3 h).

Figure 5. *rbp2* is the only RRM domain containing protein that functions in the circadian clock. A) Schematic representation of the domain structure of the three Rbp proteins in *S. elongatus*. Black bars represent the RRM domain, vertical lines represent the glycine-rich domain found only on Rbp1, and an open box represents the conserved "PDPRWA" motif found at the C-terminus of Rbp3. B) Bioluminescence output, in counts per second, from a P$_{kaiB}$-*luc* reporter. Deletion of *rbp2* results in long-period rhythms of gene expression (triangles, 26.1 ± 0.3 h), whereas rhythms after deletion of *rbp1* (squares, 25.1 ± 0.4 h) or *rbp3* (diamonds, 24.5 ± 0.4 h) are similar to the WT (closed circles, 24.7 ± 0.4 h). WT is AMC2036. C) Table reporting the period $\pm$ standard deviation of *rbp* double mutants, calculated from bioluminescence traces from a P$_{kaiB}$-*luc* reporter. WT is AMC541.

Figure 6. RNA binding activity of Rbp2 is likely required to execute circadian functions. A) Homology model of Rbp2 bound to RNA. Rbp2 (green), RNA binding domains RNP-2 (blue) and RNP-1 (yellow). RNP-1 aromatic residues R42-F44-F46 known to be important for RNA binding and Y4 located in RNP-2. Position Y4 is shown in red. B) Bioluminescence output, in counts per second, from a P$_{kaiB}$-*luc* reporter. Mutations that likely impair RNA binding *rbp2-Y4A* (yellow cross) and *rbp2-R42A-F44A-F46A* (purple diamonds) confer a long-period rhythm of

gene expression, similar to a *rbp2* deletion (red squares), compared to WT (blue circles) or the complemented strain (green triangles). WT is AMC2036.

Figure 7. Lack of Rbp2 and KaiC complex formation *in vitro* suggests an indirect association. Chromatograms of gel filtration analysis showing the elution profiles of A) Rbp2 only, B) KaiC only and C) KaiC and Rbp2 together demonstrate a Rbp2-KaiC complex is not formed. Chromatograms of gel filtration analysis of D) poly(rU) homopolymer only, E) Rbp2 and poly(rU), F) KaiC and poly(rU) or G) KaiC and Rbp2 and poly(rU)suggest that the presence of RNA does not promote Rbp2-KaiC complex formation. However, a new peak that eluted earlier on the chromatogram (E,) labelled with black arrow was observed when Rbp2 was incubated with poly(rU), indicating the formation of a larger complex and confirming the ability of Rbp2 to bind RNA.

SUPPLEMENTAL MATERIAL

SUPPLEMENTAL TEXT

Identification of polar CATs. In an attempt to identify proteins that are involved in localizing and maintaining proteins at the bacterial cell poles, termed by us as polar CATs (Coordinators/Anchors/ Transporters), we took advantage of a genetic reporter assay described previously (Fixen et al., 2012). The screen is based on fusing the cyclic-AMP receptor protein (CRP), which does not localize to the cell poles, to a polar protein and expressing it in an *E. coli* strain deleted for the *crp* gene. Because transcription of the maltose regulon genes is positively regulated by CRP, cells in which the CRP fusion protein is sequestered at the pole via the polar protein moiety exhibit a maltose negative phenotype, while cells expressing just the CRP remain maltose positive.

To identify polar CATs, we fused CRP to the general phosphotransferase system (PTS) protein enzyme I (EI), a soluble protein previously shown to localize to negatively curved membrane regions at the poles of *E. coli* cells (Govindarajan, Elisha, Nevo-Dinur, & Amster-Choder, 2013). Only the C-terminal domain of EI (EI'), which is sufficient for EI polar targeting (Lopian, Elisha, Nussbaum-Shochat, & Amster-Choder, 2010), was fused to CRP and the EI'-CRP fusion protein was expressed from a plasmid in MG1655 Δ*crp E. coli* cells. Cells expressing CRP alone served as a control, and both strains were plated on MacConkey maltose plates. While MG1655 Δ*crp* cells expressing just CRP formed red colonies (maltose positive phenotype), MG1655 Δ*crp* cells expressing EI'-CRP grew as white colonies (maltose negative phenotype) (Supplementary Figure 1A), confirming that EI' sequesters CRP at the poles.

To identify genes encoding polar CATs, which are involved in polar localization of EI'-CRP and, hence, their inactivation would generate a maltose positive phenotype, we subjected the chromosome of MG1655 Δ*crp* cells expressing EI'-CRP to transposon mutagenesis, using

the EZ-Tn5™<KAN-2>Tnp Transposome™ Kit (Illumina). We isolated 16 maltose positive

mutants and identified the genes into which the transposon was inserted by Vectorette PCR

(Arnold & Hodgson, 1991). In 10 of the mutants identified the transposon inserted into the

sequence encoding the EI' moiety of the fusion protein. Using the lambda red recombination

system (Datsenko & Wanner, 2000), we replaced each of the 6 remaining genes that generated

the maltose-positive phenotype with a chloramphenicol-resistance cassette. Polar localization of

EI-mCherry, expressed from a plasmid, was disrupted only in $\Delta evgS$, and $\Delta ycaN$ strains

(Supplementary Figure 1B). When fused to a monomeric GFP, EvgS and YcaN localized to the

cell poles (Supplementary Figure 2A). When expressed together with EI-mCherry, EvgS and

YcaN were found to co-localize with EI (Supplementary Figure 2B). Hence, EvgS and YcaN

were defined as polar CATs that are involved in EI polar localization.

SUPPLEMENTAL MATERIALS AND METHODS

Identification of Polar CATs

Materials: Primers used

S.No	Primer	Sequence
1	F-EI-BamHI	CGGATCCATGATTTCAGGCATTTTAGC
2	R-EI-NotI	GCGAGCGGCCGCGATTGTTTTTTCTTCAATGAAC
3	F-mGFP_XmaI_C	CAGCCCGGGATGAGTAAAGGAGAAGAACTTTTCACTGG
4	R-mGFP_PstI_C	GACTGCAGttaTTTGTATAGTTCATCCATGCCATGTG
5	F-BamHI_evgS	GGGATCCACATGAAGTTTTTACCCTATATTTTTCTTCTC

6	R-KpnI_*evgS*	GGGTAACGGTCATTTTTCTGACAGAAAACAGCAATC
7	F-BamHI_ycaN	GGGATCCACATGCGGATGAATATGTCTGACTTTG
8	R-KpnI_ycaN	CTGGTACCGTTGTGGTCGGTGACGCTG
9	F_KO_*evgS*	ACTGATGGATCTTTACACATTCGCACAACGTAACAAAATCGGCTAACCACGTGTAGGCTGGAGCTGCTTC
10	R_KO_*evgS*	GATGTGCTGGTAAATAGCTCCCACATTTGAACATTGTGGGAGCCGCTATATGGGAATTAGCCATGGTCC
11	F_KO_*ycaN*	AATCCTGTAAACGTGATGATTCAGGATGAGTTAATGAAGGATTTTCACTAGTGTAGGCTGGAGCTGCTTC
12	R_KO_*ycaN*	GATTAGGACTGATATTCCCGCTGCTGGCGCGTAAAGCGAATAGTAAATAAATGGGAATTAGCCATGGTCC

Methods: The plasmid p-*ptsI-crp*, which encodes a translational fusion of EI to CRP, was created from the p-*cheZ*::*crp* (Fixen et al., 2012) vector in two steps. In the first step, *cheZ* was removed from the vector using the enzymes BamHI and NotI. The *ptsI* gene, which encodes EI, was amplified with primers F-EI-BamHI and R-EI-NotI and ligated to the cleaved vector. In the second step, the Kan^R antibiotic resistant cassette was replaced with a Cm^R cassette in the following way: *neoR* required for KanR was removed, using the enzymes AatII and SpeI. The *cat* gene, which confers CM^R, was taken from pZA31 (lab collection), which was digested with AatII and SpeI. This CM^R encoding fragment was ligated to the cleaved vector to construct pEI-CRP.

The plasmids encoding in-frame translational fusions of EvgS or YcaN to mGFP were constructed in two steps. In the first step, mGFP was amplified from pAR100 (Govindarajan et al.,

2013), using the primers F-mGFP_XmaI_C and R-mGFP_PstI_C, and ligated to pQE32-lacIQ (Lopian et al., 2010) cleaved by PstI and XmaI, thus creating pQE-mGFP. In the second step, the *evgS* or *ycaN* open reading frames were amplified with primers F-BamHI_*evgS* and R-KpnI_*evgS* or F-BamHI_ycaN and R-KpnI_ycaN, respectively, and ligated to pQE-mGFP cleaved with BamHI and KpnI, thus creating pQE-evgS-mGFP or pQE-ycaN-mGFP, respectively.

Chromosomal knockouts Δ*evgS*::Cm and Δ*ycaN*::Cm were created by the λ-red recombination method (Datsenko & Wanner, 2000), using primers F_KO_evgS & R_KO_evgS and F_KO_ycaN and R_KO_ycaN, respectively. The plasmid expressing EI-mCherry was described previously in (Govindarajan et al., 2013).

SUPPLEMENTAL FIGURE LEGENDS

Supplemental Figure 1. EvgS and YcaN fused to EI confer a maltose negative phenotype.

(A) Maltose utilization capability of cells expressing CRP or EI-CRP tested on MacConkey-maltose plates. Colonies of MG1655 Δ*crp* cells expressing CRP or an EI-CRP fusion protein formed red (upper panel) or white (lower panel) colonies, respectively.

(B) Fluorescence microscopy images showing the subcellular distribution of EI-mCherry expressed from a plasmid in wild-type cells compared to mutant cells harboring chromosomal deletions of *evgS*, or *ycaN*.

Supplemental Figure 2. The polar CATs EvgS and YcaN co-localize with EI at the cell poles.

(A) Images showing polar localization of EvgS and YcaN, fused to mGFP. (B) Fluorescence microscopy images showing co-localization of EI-mCherry expressed from the chromosome (red) with mGFP-tagged EvgS or YcaN expressed from a plasmid (green) in *E. coli*.MG1655 cells. Scale bar corresponds to 2 μm.

Supplemental Figure 3. Disruption of SynPCC7942_0417 or *rbp2* results in altered circadian rhythms of gene expression. Bioluminescence output, in counts per second, from a P$_{kaiB}$-*luc* reporter. Disruption of SynPCC7942_0417 (▼0417) or SynPCC7942_1999 (Δ*rbp2*) results in a long-period rhythm of gene expression. ▼0417 purple squares, 25.3 ± 0.7 h, Δ*rbp2* green circles, 26.7 ± 0.4 h compared to WT, blue triangles, 24.44 ± 1.3 h. WT is AMC2158 transformed with pAM5428 (Δ*kaiC*) and pAM5081 (YFP-KaiC).

Table S1. Cyanobacterial strains used in this study

Strain	Genotype	Antibiotics	Source
AMC2036	P$_{kaiB}$-*luc* reporter in NS3	Cm	(Cohen et al., 2014)
AMC2158	P$_{kaiB}$-*luc* reporter in NS3	Nt	(Cohen et al., 2014)
AMC541	P$_{kaiB}$-*luc* reporter in NS2	Cm	(Ditty, Canales, Anderson, Williams, & Golden, 2005)
AMC704	Δ*kaiC* in-frame deletion in AMC541	Cm	(Ditty et al., 2005)

Table S2. Plasmids used in this study

Plasmid	Description	Antibiotic Resistance	Source
pAM5080	P$_{trc}$-*yfp-kaiC* expressed in NS2	Km	(Cohen et al., 2014)
pAM5081	P$_{trc}$-*yfp-kaiC* expressed in NS1	SpSm	(Cohen et al., 2014)
pBM1	P$_{trc}$-*yfp-kaiC-CII* domain only, modified from pAM5080	Km	This work
pBM3	P$_{trc}$-*yfp-kaiC-CI* domain only, modified from pAM5080	Km	This work
pBM7	P$_{trc}$-*yfp-kaiC*^{E77Q,E78Q} modified from pAM5080	Km	This work
pBM23	P$_{trc}$-*yfp-kaiC-CI*$^{R40A, K172A}$ domain only, modified from pAM5080	Km	This work
pBM24	P$_{trc}$-*yfp-kaiC*^{T42S} modified from pAM5080	Km	This work
pBM25	P$_{trc}$-*yfp-kaiC*^{S157P} modified from pAM5080	Km	This work
pBM26	P$_{trc}$-*yfp-kaiC*^{A251V} modified from pAM5080	Km	This work
pBM27	P$_{trc}$-*yfp-kaiC*^{R393C} modified from pAM5080	Km	This work
pBM28	P$_{trc}$-*yfp-kaiC*^{F470Y} modified from pAM5080	Km	This work

pAM5095	P$_{trc}$-*yfp-kaiC^{AA}* expressed from NS2, modified from pAM5080	Km	(Cohen et al., 2014)
pAM5096	P$_{trc}$-*yfp-kaiC^{AE}* expressed from NS2, modified from pAM5080	Km	(Cohen et al., 2014)
pAM5428	Deletion of *kaiC* (Δ*kaiC)*	Gm	This work
4F7-W4	Mu insertional mutation into *minC* (▼*minC*)	Cm	(Holtman et al., 2005)
4G8-FFF4	Mu insertional mutation into SynPCC7942_1816	Cm	(Holtman et al., 2005)
7E6-LL2	Mu insertional mutation into SynPCC7942_0417 (▼0417)	Cm	(Holtman et al., 2005)
8S30-A12	Tn*5* insertional mutation into SynPCC7942_1310	Km	(Holtman et al., 2005)
10B12-E5	Mu insertional mutation into *minD2* (▼*minD2*)	Cm	(Holtman et al., 2005)
pSC162	Deletion of *minD1* (Δ*minD1*)	Nt	This work
pSC192	Deletion of *rbp2* (Δ*rbp2*)	Km	This work
pLA0004	P$_{trc}$-*rbp2*-strep expressed from NS1	SpSm	This work
pLA0007	Deletion of *rbp3*(Δ*rbp3*)	SpSm	This work
pLA0009	Deletion of *rbp1*(Δ*rbp1*)	Gm	This work
pLA0012	P$_{rbp2}$-*rbp2* expressed from NS1	SpSm	This work
pLA0019	P$_{rbp2}$-*rbp2^{Y4A}* expressed from NS1	SpSm	This work
pLA0017	P$_{rbp2}$-*rbp2$^{R42A-F44A-F46A}$* expressed from NS1	SpSm	This work

Table S3. Proteins identified to interact specifically with either diffuse or polar KaiC.

Essentiality determined by (Rubin et al., 2015).

SynPCC7942_	gene	KaiC associated	tested
0001	*dnaN*	localized	No, essential
0417		localized	Yes
0473		localized	Yes
0507	*frr*	localized	No, essential
0537	*fabF*	localized	No, essential
0694	*rps1*	localized	No, essential
0700		localized	Yes
0805		localized	Yes
1081		localized	No, essential
1379	*accC*	localized	No, essential
1426	*rbcL*	localized	No, essential
1501	*serA*	localized	Yes
1552	*ilvC*	localized	No, essential

1743	*ndhH*	localized	No, essential
1999	*rbp2*	localized	Yes
2220	*rplE*	localized	No, essential
2530	*rpsB*	localized	No, essential
2230	*rplW*	localized	No, essential
2257		localized	Yes
2349	*pilT*	localized	Yes
2477	*sulA*	localized	Yes
2530	*rpsB*	localized	No, essential
2541	*rplS*	localized	No, essential
0012	*rpsF*	diffuse	No, essential
0204		diffuse	No
0318		diffuse	No
1232	*petC*	diffuse	No, essential
1314	*ftsH*	diffuse	Yes
1476		diffuse	Yes
2378	*ftsZ*	diffuse	No, essential

Figure 1

A YFP-KaiC
2.5 μm

B YFP-CI
2.5 μm

C YFP-CII
2.5 μm

D YFP-CI-monomer
2.5 μm

Figure 2

Figure 3

A 30°C

B 42°C

C control

D + nisin

E + DNP

F ▼SynPCC7942_1310

G▼SynPCC7942_1816

H ▼*minC*::*Mu*

I Δ*minD1*::Nt

J ▼*minD2*::*Mu*

K Δ*minD1*::NAT,
▼*minD2*::Cm

Figure 4

Figure 5

A

Rbp1
Rbp2
Rbp3
PDPRWA

B

	WT	Δ*rbp2*	Δ*rbp1*	Δ*rbp3*
	24.7 ± 0.4	26.1 ± 0.3	25.1 ± 0.4	24.5 ± 0.4

Bioluminesce (cps)

Hours in LL
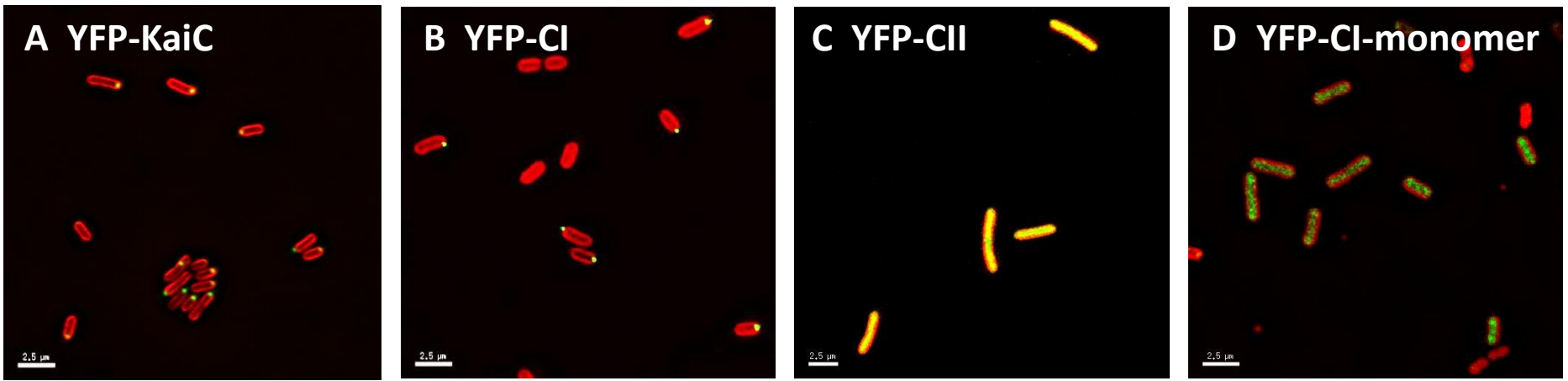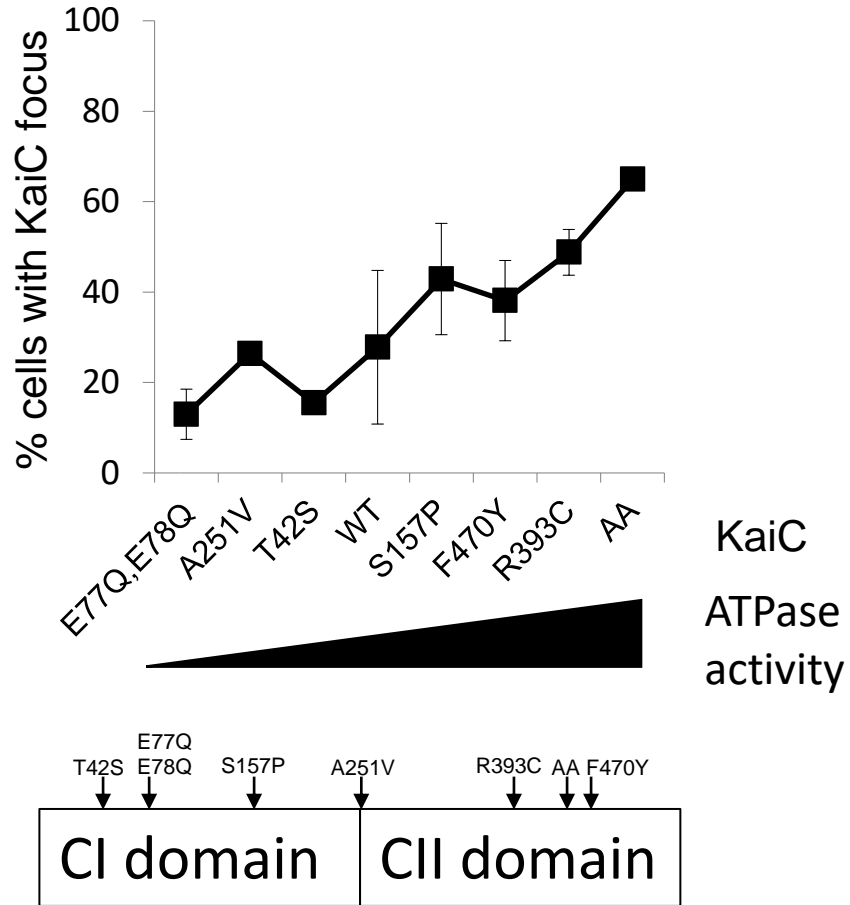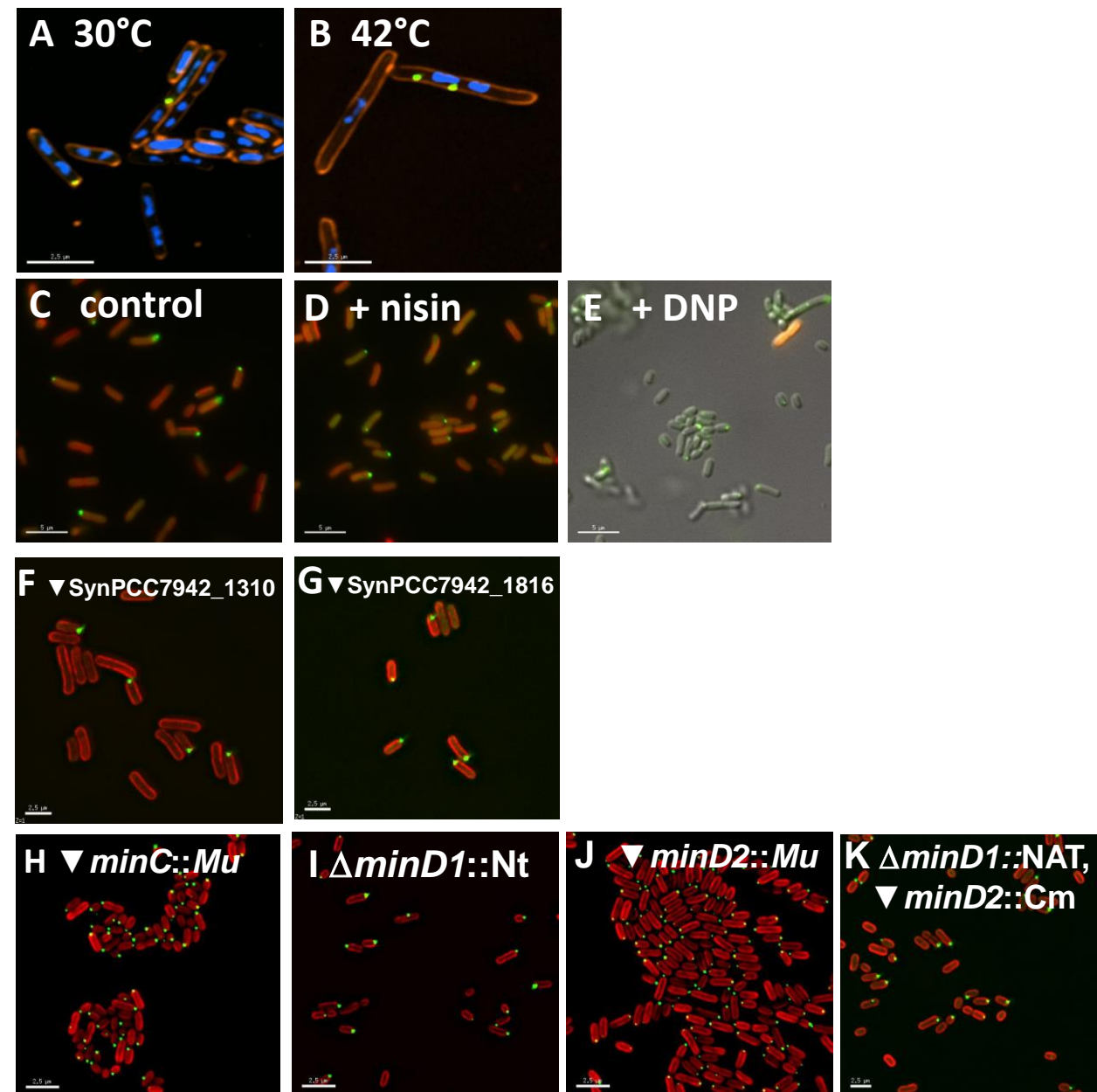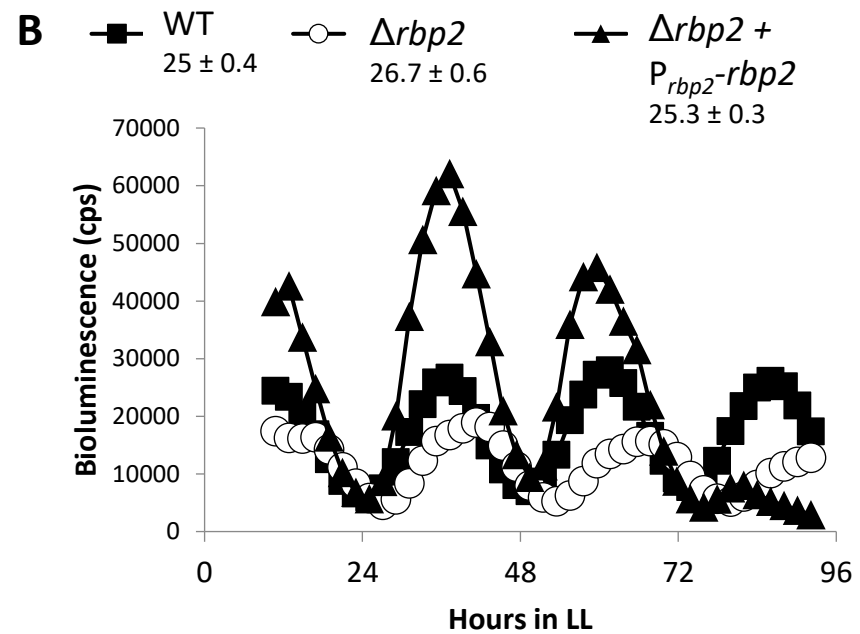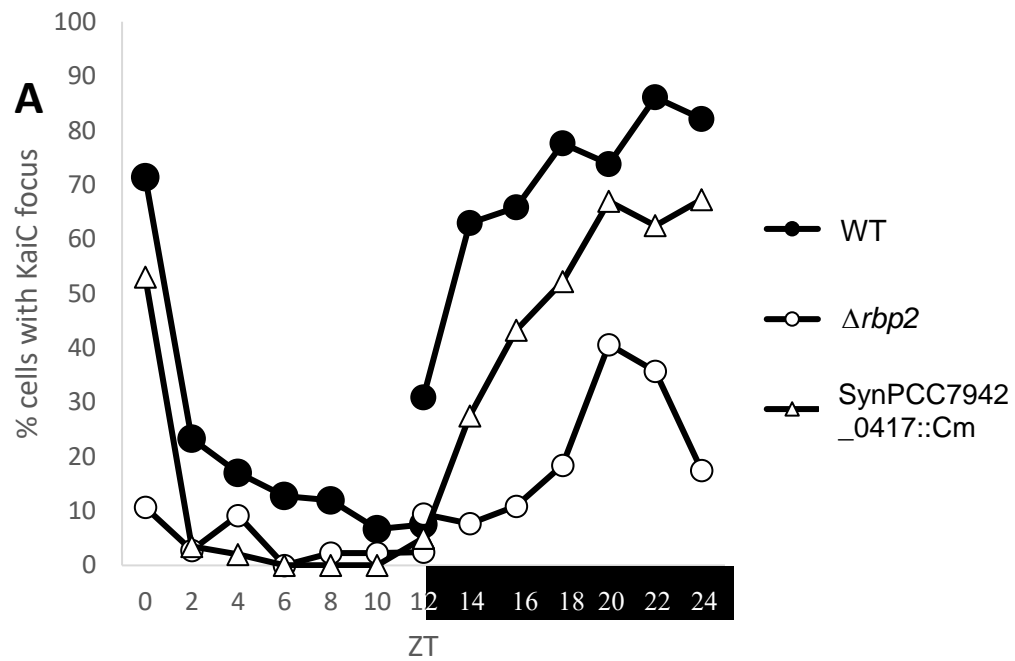
C

Strain	Period (h)
WT (AMC541)	25.2 ± 0.1
Δ*rbp1* Δ*rbp2*	26.4 ± 0.4
Δ*rbp1* Δ*rbp3*	25.2 ± 0.3
Δ*rbp2* Δ*rbp3*	26.2 ± 0.3

Figure 6

A

B

WT
25.1 ± 0.2

Δ*rbp2+rbp2*
25.2 ± 0.3

Δ*rbp2+rbp2-R42AF44AF46A*
26.4 ± 0.4

Δ*rbp2+rbp2-Y4A*
26.2 ± 0.2

Δ*rbp2*
26.1 ± 0.4
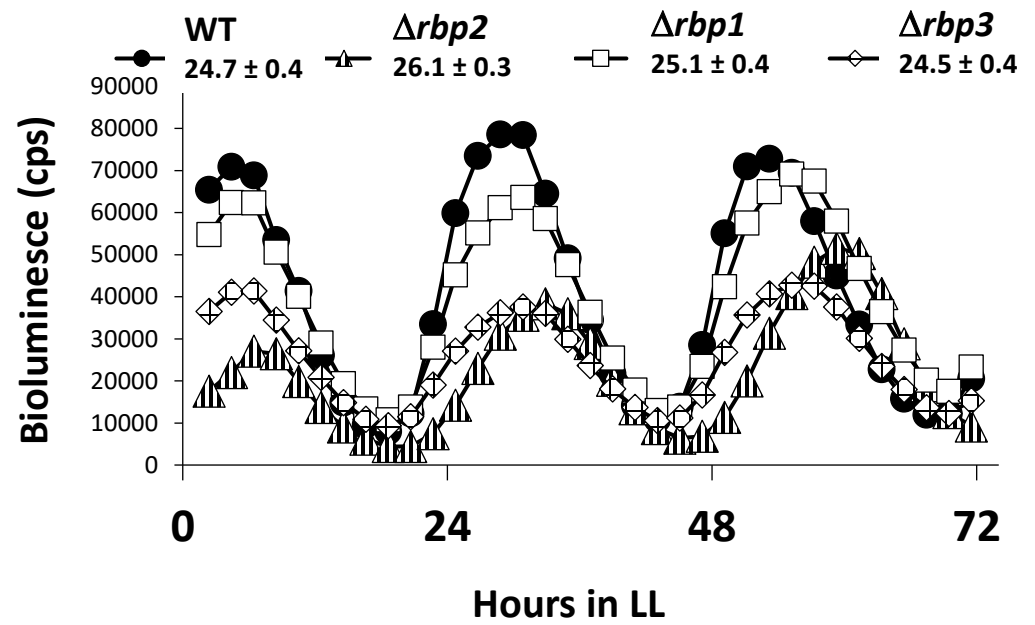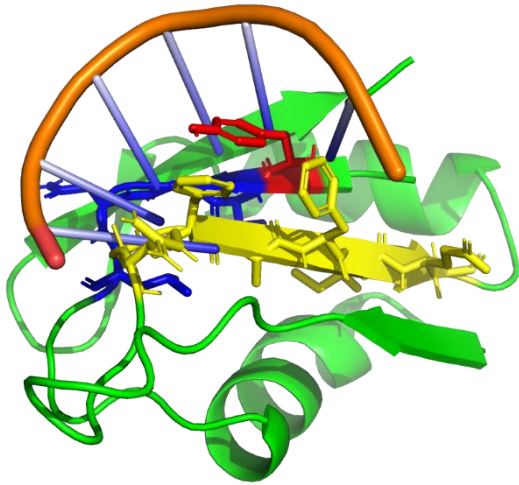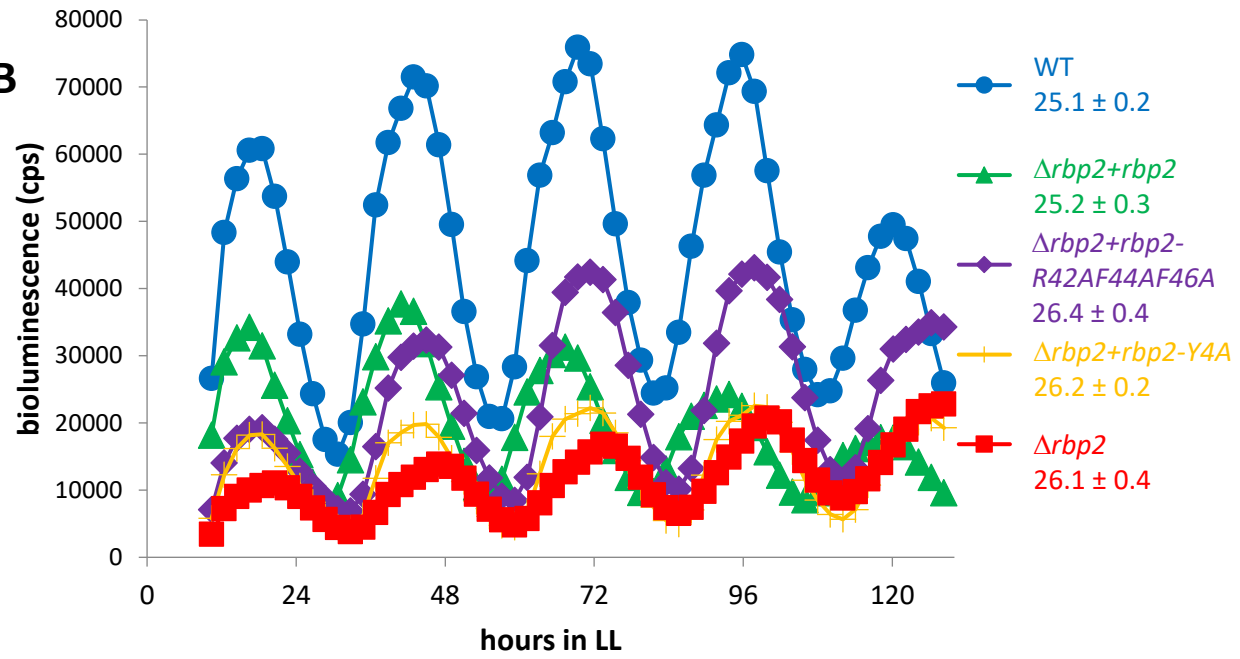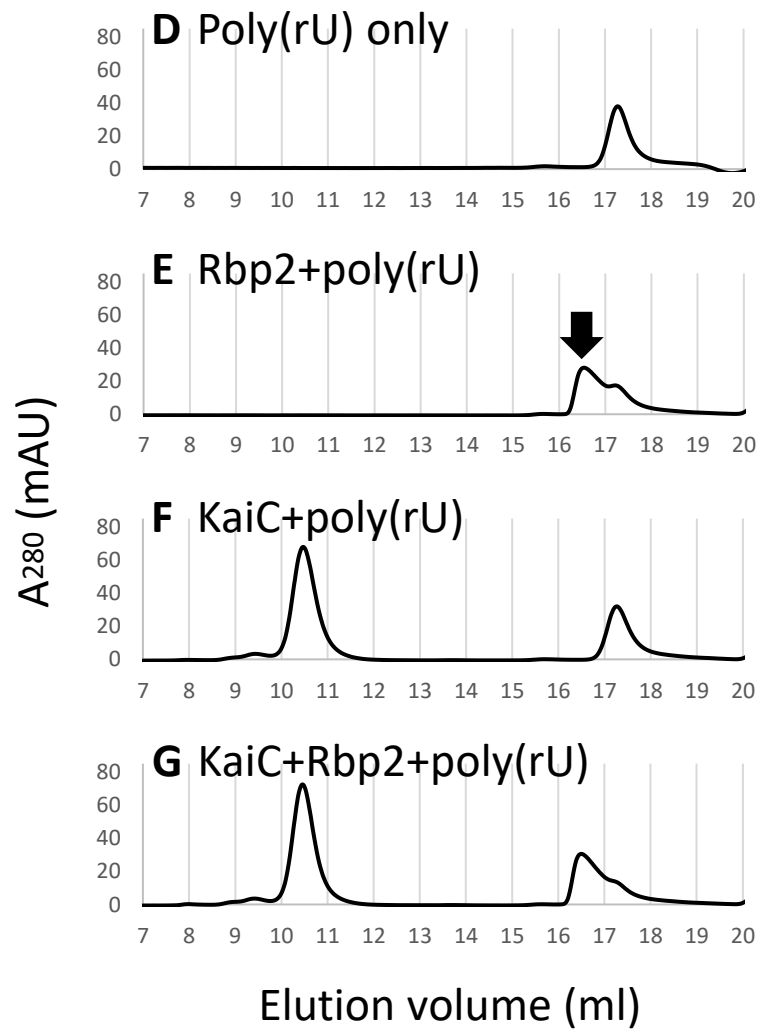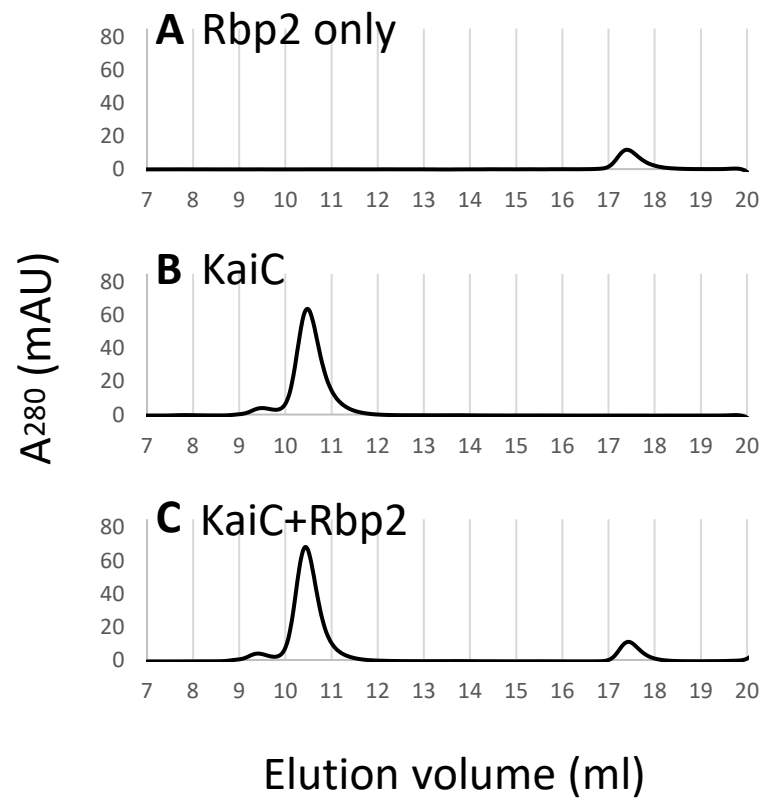
Figure 7

Supplemental Figure 1

A

MG*Δcrp* + pCRP
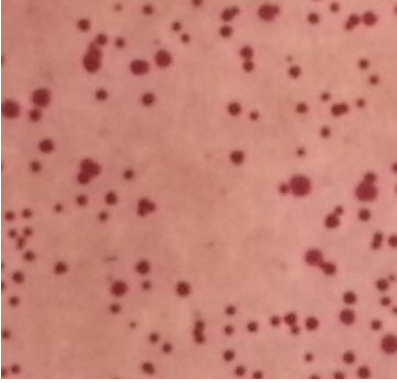
MG*Δcrp* + pEI-CRP

B
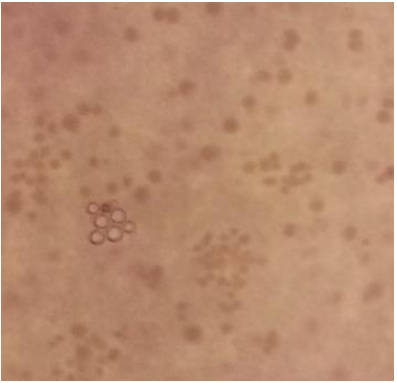
Wild type

Δ*evgS*::CM

Δ*ycaN*::CM

EI-mCherry (expressed from plasmid)
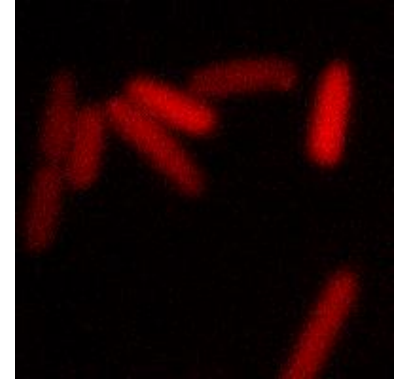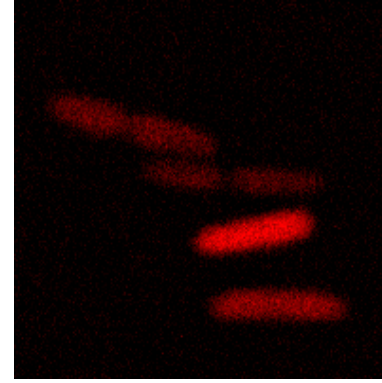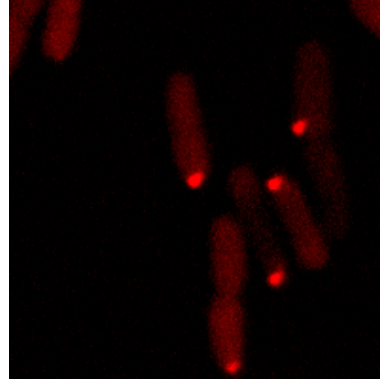
Overlay
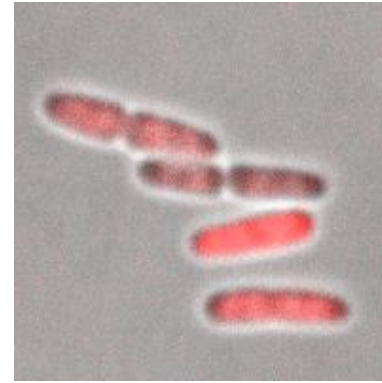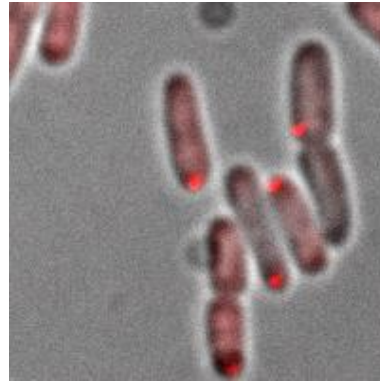
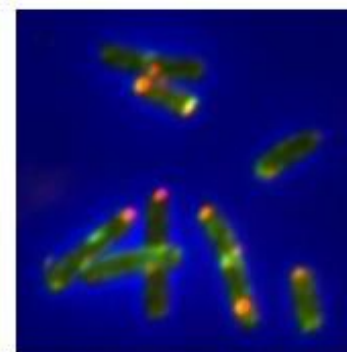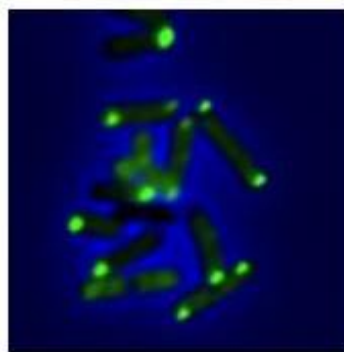**Supplemental Figure 2**

A
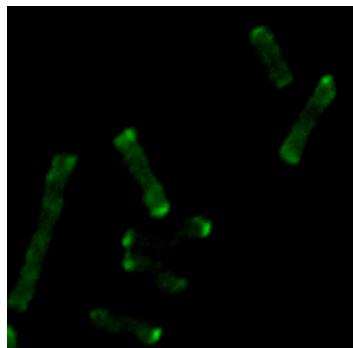
EvgS-mGFP   Overlay
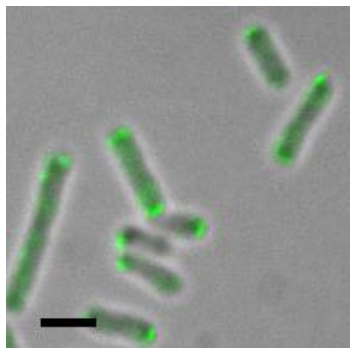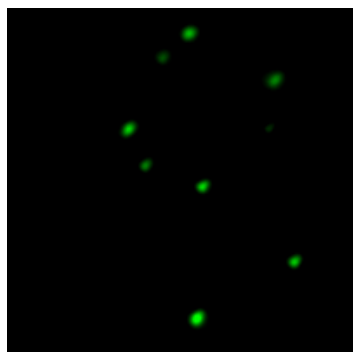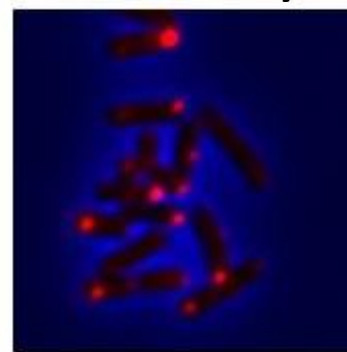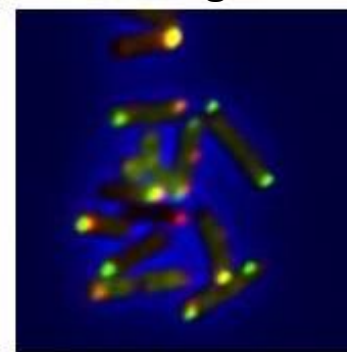
YcaN-mGFP   Overlay
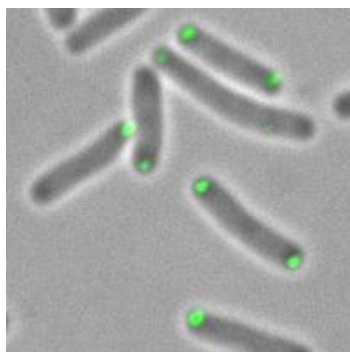
B
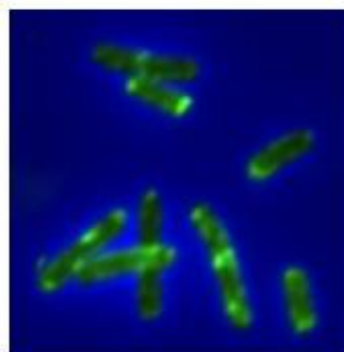
EvgS-mGFP   EI-mCherry   Merge
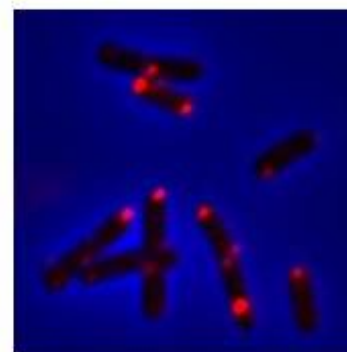
YcaN-mGFP   EI-mCherry   Merge

Supplemental Figure 3